NSWC/WOL TR 77-96

DDT BEHAVIOR OF WAXED MIXTURES OF RDX, HMX, AND TETRYL

BY DONNA PRICE and RICHARD R. BERNECKER

RESEARCH AND TECHNOLOGY DEPARTMENT

18 OCTOBER 1977

Approved for public release; distribution unlimited.

NAVAL SURFACE WEAPONS CENTER

Dahlgren, Virginia 22448 • Silver Spring, Maryland 20910

UNCLASSIFIED

SECURITY CLASSIFICATION OF THIS PAGE (When Data Entered)

REPORT DOCUMENTATION PAGE

READ INSTRUCTIONS BEFORE COMPLETING FORM

1. REPORT NUMBER: NSWC/WOL/TR-77-96
2. GOVT ACCESSION NO.
3. RECIPIENT'S CATALOG NUMBER
4. TITLE (and Subtitle): DDT Behavior of Waxed Mixtures of RDX, HMX, and Tetryl
5. TYPE OF REPORT & PERIOD COVERED
6. PERFORMING ORG. REPORT NUMBER
7. AUTHOR(s): Donna Price [redacted] Richard R. Bernecker
8. CONTRACT OR GRANT NUMBER(s)
9. PERFORMING ORGANIZATION NAME AND ADDRESS: Naval Surface Weapons Center, White Oak Laboratory, White Oak, Silver Spring, Maryland 20910
10. PROGRAM ELEMENT, PROJECT, TASK AREA & WORK UNIT NUMBERS: 61152N; ZR00001; ZR0130901; a. WR0119; SF33354316; b. SSP077402;
11. CONTROLLING OFFICE NAME AND ADDRESS
12. REPORT DATE: 18 Oct [redacted] 77
13. NUMBER OF PAGES: 64 (12 6 7p.)
14. MONITORING AGENCY NAME & ADDRESS (if different from Controlling Office)
15. SECURITY CLASS. (of this report): Unclassified
15a. DECLASSIFICATION/DOWNGRADING SCHEDULE

16. DISTRIBUTION STATEMENT (of this Report)

Approved for public release; distribution unlimited.

16 ZR00001, F33354

17. DISTRIBUTION STATEMENT (of the abstract entered in Block 20, if different from Report)

17 ZR0130901, SF33354316

18. SUPPLEMENTARY NOTES

19. KEY WORDS (Continue on reverse side if necessary and identify by block number)

DDT	HMX/wax	Flame Spreading
Detonation	RDX/wax	
Sensitivity	Tetryl/wax	
Explosives	Combustion	

391 596

20. ABSTRACT (Continue on reverse side if necessary and identify by block number)

DDT data are presented for the 94/6 RDX/wax series over 70% to 97% TMD. The trends are similar to those of the 91/9 RDX/wax series but this mixture has a much shorter time range corresponding to its increased sensitivity. Data are also given for one waxed RDX and two waxed HMX series at fixed percent porosity (100 - % TMD). . 1 mixtures followed the physical model proposed for DDT of 91/9 RDX/wax. However, the series run at fixed % TMD and varying wax content showed strong correlations between the relative time to detonation and the predetonation column length. (Cont.)

DD FORM 1 JAN 73 1473 EDITION OF 1 NOV 68 IS OBSOLETE
S/N 0102-LF-014-6601

UNCLASSIFIED
SECURITY CLASSIFICATION OF THIS PAGE (When Data Entered)

(20) No similar correlation appears at fixed composition and varying porosity.

NSWC/WOL TR 77-96 18 October 1977

DDT BEHAVIOR OF WAXED MIXTURES OF RDX, HMX, AND TETRYL.

This work was carried out under tasks ZR0130901, IR-159; SF33354316/18460 and SSPO77402. The present results and conclusions on the transition from burning to detonation of waxed granular explosives should be of interest in the area of explosive sensitivity, especially as related to the problem of premature initiation.

Julius W. Enig

JULIUS W. ENIG
By Direction

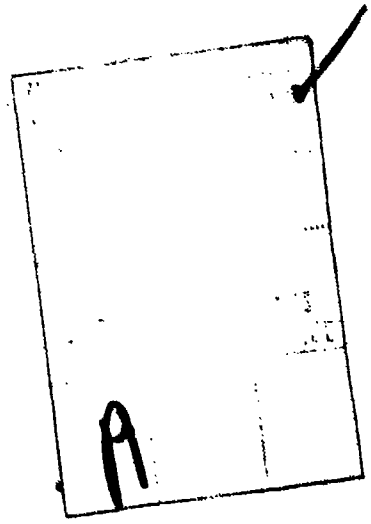

TABLE OF CONTENTS

TABLES

TABLES (CONT)

ILLUSTRATIONS

ILLUSTRATIONS (CONT)

DDT BEHAVIOR OF WAXED MIXTURES OF RDX, HMX, AND TETRYL

I. INTRODUCTION

The purpose of this report is to present the data, accumulated over a period of years, for waxed RDX and HMX as well as two shots on waxed tetryl. The work has been carried out for various reasons under various projects. For example, our initial study under IR 159 was carried out on 91/9 RDX/wax (1) and was made to help elucidate the mechanism of deflagration to detonation transition (DDT). But for gas loading of explosives (2) to examine their sensitivity to DDT, the 94/6 mixture was preferable, i.e., exhibited more useful burning characteristics and predetonation column length for the desired application. Hence, transition experiments for 94/6 RDX/wax over the compaction range of 70 - 97% theoretical maximum density (TMD) were carried out and are reported here. In addition, data for propellant models* of HMX/wax and RDX/wax at 0 - 15% wax and 70 - 85% TMD are included. Thus we shall have in a single report the DDT characterization of all the waxed explosives examined so far.

II. EXPERIMENTAL ARRANGEMENT AND PROCEDURE

The experimental configuration and procedure have been fully described in an earlier report (1). In brief, a seamless steel tube (16.27 mm ID, 50.95 mm OD) with heavy end closures was used. A B/KNO_3 ignitor (1) was used to ignite one end of the 295.4 mm explosive column.

Charge loading, tube instrumentation (ionization pins [IP] to monitor reaction fronts, and strain gages [SG] to follow internal pressure), recording equipment, circuitry, and data reduction are also as in reference 1 with the modification for strain gages given in reference 2.

1. R. R. Bernecker and D. Price, "Transition from Deflagration to Detonation in Granular Explosives", NOLTR 72-202, 13 Dec 1972.
2. R. R. Bernecker and D. Price, "Sensitivity of Explosives to Transition from Deflagration to Detonation", NOLTR 74-186, 7 Feb 1975.

*These propellant models are also explosive models, and, in general, propellants are a subclass of explosives.

Chemical materials used for the charges were RDX (834; Class D, $\bar{\delta}$ ∿ 850μ), RDX (597; Class A, $\bar{\delta}$ ∿ 200μ), HMX (689*; Class A, $\bar{\delta}$ ∿ 200μ), RDX (659; Class E, $\bar{\delta}$ ∿ 15μ), tetryl (812; $\bar{\delta}$ ∿ 470μ), carnauba wax (134; $\bar{\delta}$ ∿ 125μ). The mixing procedure was that used in reference 1 for 1 kg batches. When a screen cut of $\bar{\delta}$ ∿ 115μ was used, it was obtained by taking the fraction passing through a 125μ sieve opening and retained on a sieve of 105μ opening.

III. EXPERIMENTAL RESULTS AND DISCUSSION

A. 94/6 RDX/Wax

Detailed data and records for the shots made with 94/6 RDX/wax are given in Appendix A. Table 1 contains a summary of the data and Figures 1 and 2 show, respectively, the effect of porosity on predetonation column length (ℓ) and various predetonation times as defined in Table 1.

In addition to providing information about the transitional behavior of 94/6 RDX/wax, the shots of Table 1 were designed to determine the most satisfactory of three DDT tubes. These were tubes prepared from a. AISI 1215 bar steel, b. AISI 1018 seamless tubing and c. AISI 1018 bar steel. The 1215 steel was discarded after several shots because it fragmented into pieces too small to provide any measure of ℓ. Since there was no difference in the preparation cost starting with either rod or tubing, the DDT tubes for all subsequent shots have been prepared from 1018 bar steel. Tubes prepared from the 1018 steel in earlier work had clearly indicated an ℓ value generally in good agreement with that obtained from ionization probe records. This difference in confining tubes has been pointed out in case it might have had a small effect on the results.

Figures 1 and 2 show qualitative trends very similar to those found in the DDT study of 91/9 RDX/wax (1), as would be expected. In both cases, ℓ shows an apparent minimum. The minimum appears to be at 90% TMD for 9% wax and at 82% TMD for 6% wax (Figure 1). However, the scatter of data is large and no charges were fired at 71 - 81% TMD in the present study. Hence no firm difference in location can be established. Finally, the range in ℓ (120 - 280 mm in the 9% wax mixture) has been considerably reduced here to 80 - 140 mm. This is to be expected with the increased sensitivity caused by a decrease in wax content. In the case of no wax, as shown in Section IIIC, the lower limit is about 40 mm in our apparatus.

*Smaller lots taken at different times from this batch were designated 900 and 906.

Table 1. Summary of DDT Shots on 94/6 RDX/wax

Shot No.	Batch	ρ_o g/cc	% TMD	B[a] mm/μs	$2C^a \times 10^3$ mm/μs^2	V_{PC} mm/μs	D mm/μs	ℓ mm	DDT tube from	Fragment & Probe Data Agree?	$^{41}\Delta t_D$[b] μs	$^{41}\Delta t_p$[b] μs	$^{41}\Delta t_E$[b] μs
214*	759	1.21	70.3	0.355	0.826	-	6.59	135	1018 tube	yes	182	-	-
401	759	1.21	70.3	0.322	0.549	0.92	6.24	130	1018 tube	yes	186	97	89
502	759	1.40	81.5	0.455	0.476	0.95	7.26	92	1018 tube	no	77	22.6	54.4
703	759	1.51	87.8	(∿.95)	-	1.62	7.97	105	1018 tube	yes	37.7	2.7	35.0
717	851	1.55	90.3	(1.03)	-	1.8-2.0	7.92	92	1215 bar	no	27.7	0	27.7
801	851	1.63	94.7	-	-	2.0	8.42	110	1215 bar	No tube data	30.5	0	30.5
914	851	1.66	96.8	(∿1.19)	-	3.1	8.38	114	1018 bar	yes	43.0	15	28.0
1501**	893	1.21	70.3	0.212	1.40	-	-	139	1018 bar		200	120	80
1712**	893	1.65	95.7					151	1018 bar				

*Reported in NOLTR 72-202 **Complete data will appear in a later report.

a. From equation for position of flame front: $x_F = A + Bt + Ct^2$; B is rate at 41 mm. When entry is in parentheses and no value is given for C, rate is computed from discharge time of first two probes only.

b. $^{41}\Delta t_D$ Time from discharge of probe at x = 41mm to onset of detonation.

$^{41}\Delta t_p$ Time from discharge of probe at x = 41mm to passage of PC wave.

$^{41}\Delta t_E = \Delta t_D - \Delta t_p$.

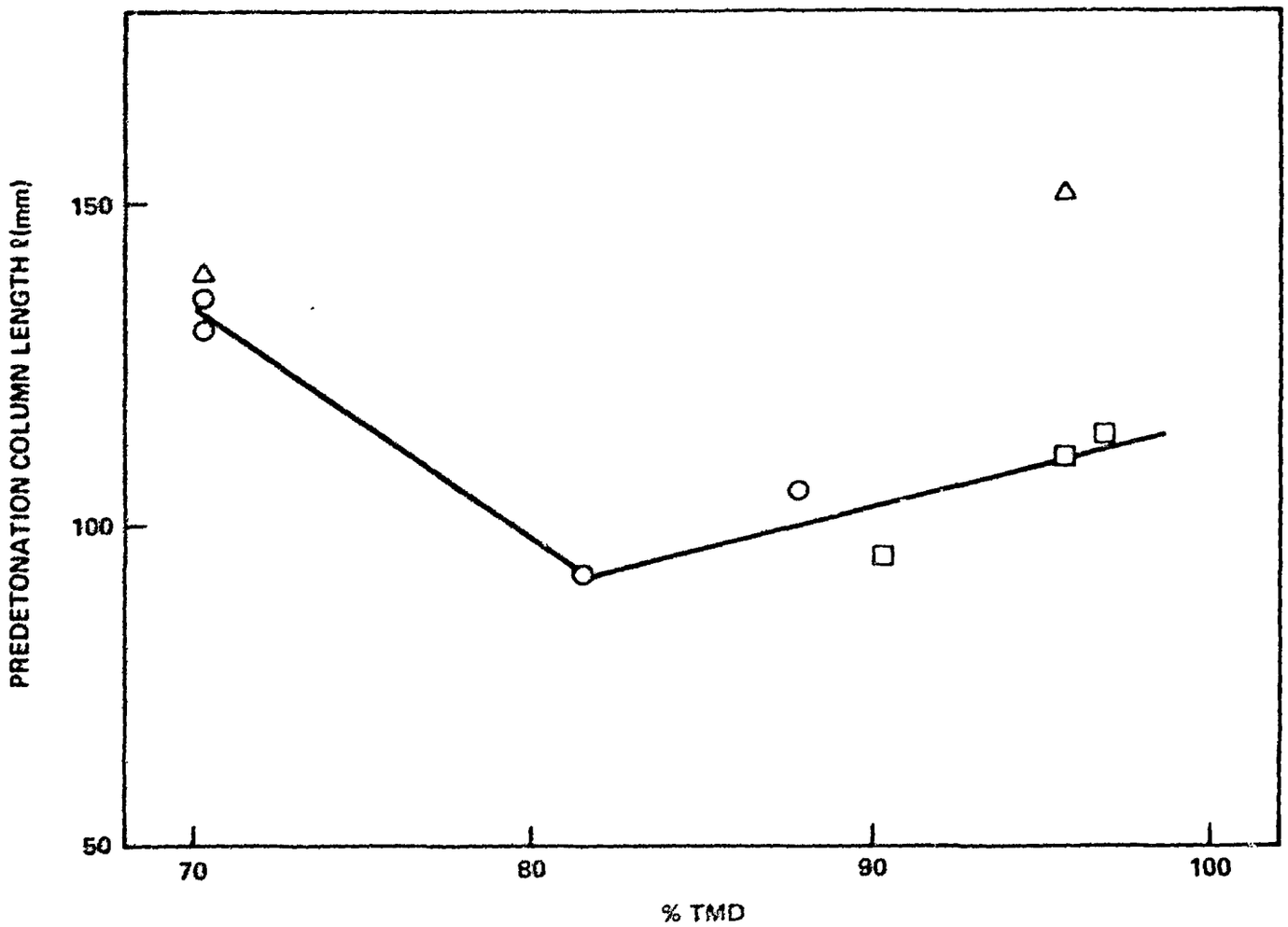

FIG. 1 EFFECT OF POROSITY ON PREDETONATION COLUMN LENGTH OF 94/6 RDX/WAX, (BATCHES: ○ 759, □ 851, △ 893).

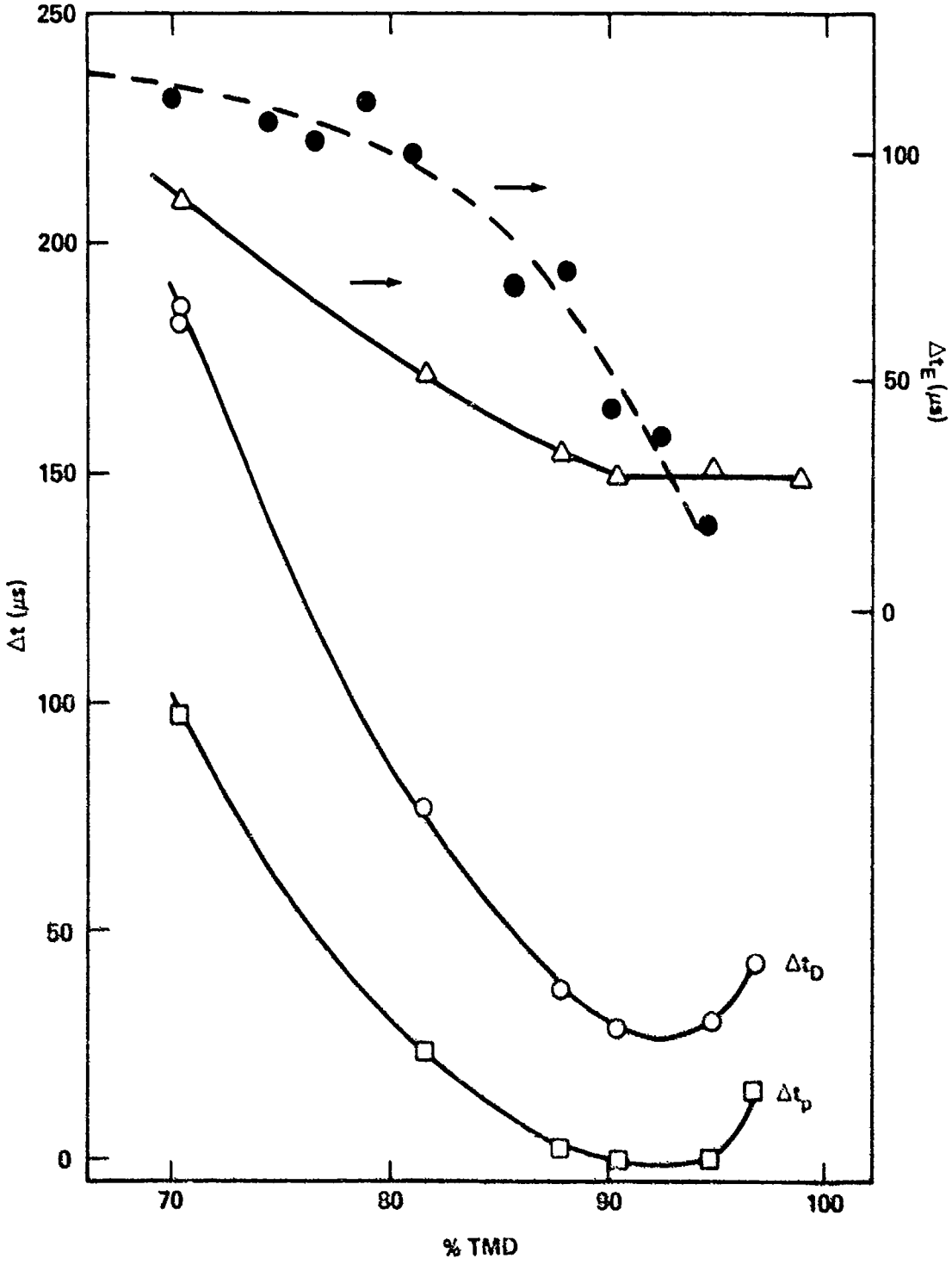

FIG. 2 EFFECT OF POROSITY ON RELATIVE PREDETONATION TIMES OBSERVED IN 94/6 RDX/WAX, (BATCHES 759 & 851; DASHED CURVE FOR 91/9 RDX/WAX).

In Figure 2, the trend for relative* time to detonation ($^{41}\Delta t_D$) is again qualitatively very similar to that exhibited by the 91/9 mix (1): decreasing with increasing % TMD. However, the earlier data show a sharp break in the curves (discontinuity of slope) and no slight increase at the high density end as do those of Figure 2. The smoother, continuous curves of Figure 2 may be a fortuitous effect of data scatter as may be the slight upturn at the high density end. Inasmuch as two charges at high % TMD were confined in slightly different steel tubes, a small difference in confinement effect on Δt could make a plateau area (no change in ℓ at 88 - 97% TMD) appear to be a minimum at 93% TMD. Although the minima of Figure 2 may be fictitious, the obvious difference between these curves and the corresponding ones for the more highly waxed RDX is, as also is the case for ℓ, the size of the range. The relative times to detonation are 63 - 610 μs for 91/9 RDX/wax; 50 - 170 μs for 94/6 RDX/wax. The respective relative times to formation of the post-convective (compressive) wave $^{41}\Delta t_p$ are 40 - 480 μs, and 0 - 97 μs. Interestingly enough, the difference between the two, $^{41}\Delta t_E$ or relative time between formation of the PC wave at x = 41 mm and the onset of detonation, is the same order of magnitude in both cases. But the curve is convex upward for 91/9 and concave upward for 94/6 RDX/wax, with the latter $^{41}\Delta t_E$ generally the lower value. In this case, the curve for the 91/9 mixture is shown as a dashed line. It was obtained as the difference between values from the two smoothed curves, Δt_D vs %TMD and Δt_p vs %TMD. When the actual differences in the data of reference 1 are used, the curve is raised at the low porosity end and no longer crosses the curve for 94/6 RDX/wax. The general trend of decreased Δt_D, Δt_p, and Δt_E is again the effect to be expected with the increased sensitivity and burning rate caused by the lesser amount of wax.

Finally Table 1 contains data for charges from three batches of 94/6 RDX/wax; all were prepared in an identical manner from the same batches of each of the two components. The smooth curves of Figures 1 and 2 indicate that 94/6 RDX/wax batches 759 and 851 are equivalent. The check of batch 893 at 70.3% TMD again shows equivalence, but the results for a 95.7% TMD charge from this batch does not. This result will be suspect until further charges can be fired.

B. 91/9 RDX/Wax

Only a few shots have been fired with 91/9 RDX/wax since the initial report on its DDT behavior (1). The first was with an 81.3% TMD charge prepared from coarse (Class D) RDX, and the objective was to see if an initial average particle size of about 850μ would measurably change the behavior of 91/9 RDX/wax prepared from a

*Relative to discharge of an ionization pin at x = 41 mm.

regular (Class A) RDX with $\bar{\delta} \sim 200\mu$. Figure 3 shows the space-time plot for the Class D mixture; the additional data appear in Appendix B.

The coarser RDX mixture results in smaller values of Δt_D, Δt_p, and ℓ. The respective values from Figure 3 are 135μs, 50μs, and 146 mm. They can be compared with smoothed curve values for Class A RDX mixtures (1) of 205μs, 114μs, and 167 mm. The decrease is still clearly evident when the comparison is made with unsmoothed experimental values obtained from the regular mixes of approximately 81% TMD (1). Thus, changing the average particle size of the RDX in the 91/9 RDX/wax from 200μ to 850μ has increased the speed with which the 81% TMD mixture undergoes DDT. This in turn we attribute to an increase in permeability caused by the use of the coarser RDX.

A second experiment was run on the regular 91/9 RDX/wax mix at the highest density to which it could be compacted in our setup. The data for this 97% TMD charge appear in Appendix B. In the previous work (1), two shots were fired at 94.5% TMD, the highest compaction achieved at that time. One shot exhibited DDT; the other failed. The results suggested either that 91/9 RDX/wax approached some critical condition at high density or that the failure was caused by some undetected flaw in the charge preparation. The latter seems to be the case since the present charge exhibited DDT with much the same values of Δt and ℓ as those found earlier for a 94.5% TMD charge. Another shot on 91/9 RDX/wax will be reported in the appropriate series below.

C. RDX

Four charges of pure RDX were fired. They were all handpacked to 69.1% TMD (1.25 g/cc). The objectives of this work were a) to examine the particle size effect on DDT of RDX, i.e., Class A vs. Class E, and b) to ascertain if RDX followed the initially proposed model for DDT (1). Subsequently, the data were also used as the 100/0 member of the RDX/wax series. The data are summarized in Table 2 and presented in more detail in Appendix C.

These data show that the fine RDX (Class E, $\bar{\delta} \sim 15\mu$) exhibits a greater predetonation column length than does the regular RDX (Class A, $\bar{\delta} \sim 200\mu$). These results confirm the trend reported by Calzia (3) for particle size effect of RDX although whether Calzia's values came from fractional screening, grinding, or reprecipitating the RDX was not indicated. The present results also confirm the trend indicated by those of the 91/9 RDX/wax prepared with coarse RDX (see previous section).

3. J. Calzia, "Experiments on the Deflagration-Detonation Transition in Condensed Explosives," Compt Rendu 276, 1397-99, (1973).

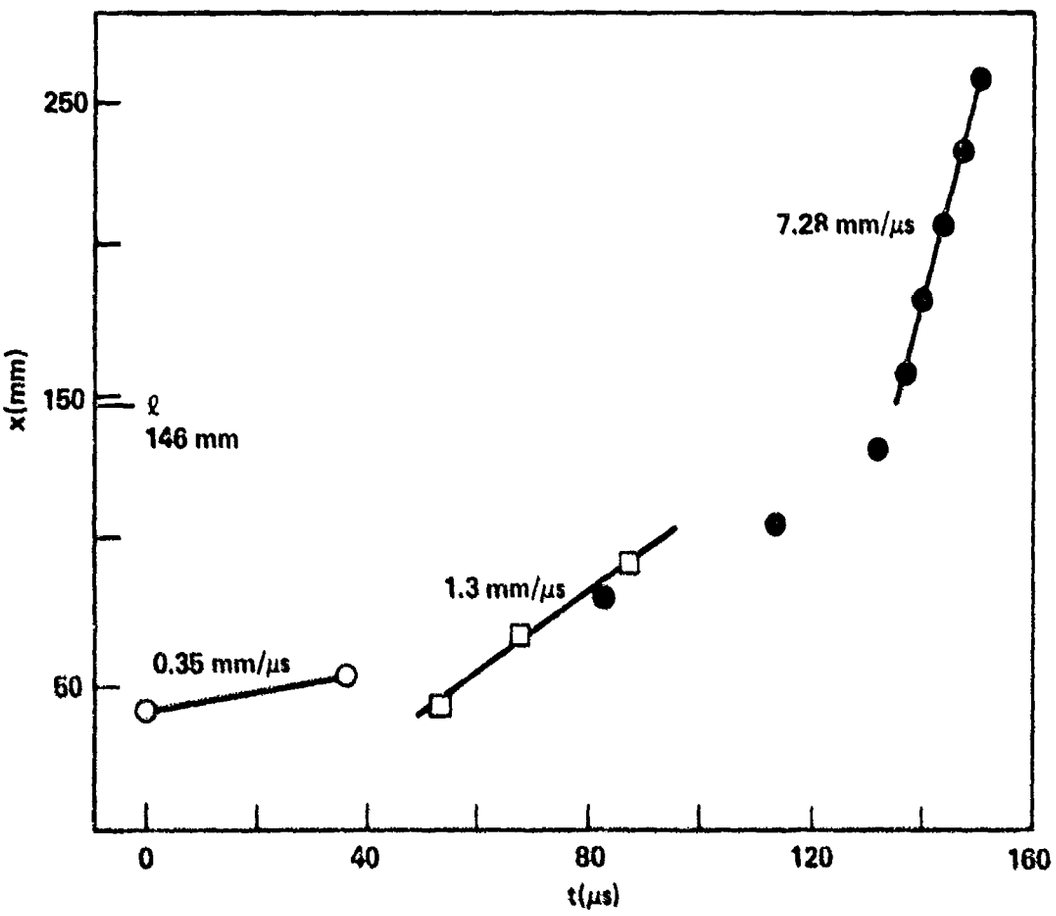

FIG. 3 SPACE-TIME PLOT FOR SHOT 603 ON 81.3% TMD 91/9 RDX (850μ)/WAX, ρ_o = 1.37 g/cc.

Table 2. Summary of RDX Shots

Shot No.*	Class RDX	Av. Particle size, μ	First velocity observed on pin records mm/μs	Predeton. column length ℓ, mm	$41_{\Delta t_D}$ μs
406	A/1	200	0.70	40	0
911	A/1	200	0.48	45	4.5
704	E/5	15	0.96	60	17
910	E/5	15	0.97	55	11

*All charges hand-packed to 1.25 g/cc or 69.1% TMD.

The data of Table 2 also show that our usual relative time of detonation (i.e., relative to discharge time of IP at 41 mm) is not of much use here. Obviously if $\ell \curvearrowright 40$ mm, we will need to have both IPs and SGs at $x < 40$ to obtain any data in the transitional area. Morever, restricting the useful experimental area to less than 40 mm means that both IP and (especially) SG locations are known to a lower percent accuracy than usual. Thus for RDX and other H.E. that exhibit DDT so readily, time and distance resolution with our instrumentation is hardly adequate. Nevertheless, we were fortunate enough to get nearly complete data in one run of the four, Shot 911 on regular RDX. The data are plotted in Figure 4.

The velocity indicated by the discharge of the first two IPs is 0.48 mm/μs. That is of the proper magnitude to be a part of an accelerating convective flame front. Similarly, the PC front velocity at 1.3 to 1.5 mm/μsec is of the size to be expected in a 70% TMD charge. (Only one of two possible PC waves was shown in Figure 4a). Hence DDT of RDX follows the same model as that initially proposed for 91/9 RDX/wax.

D. Waxed RDX, Waxed HMX Series

Tables 3 and 4 summarize the data for the RDX/wax series at 70 and 85% TMD, respectively. Detailed data and their plots are given in Appendix D. Summary plots of the effect of wax content on the predetonation column length of RDX are shown in Figure 5. At 70% TMD, the reproducibility is fair (see Figure 5a); it is probably limited at 3% wax by that of charge preparation. At 9% wax, the limitation is probably both charge preparation and the approach to a critical wax content for the experimental setup.*

The curve ℓ vs. % wax for the 70% TMD charges is approximately linear up to 6% wax; its sharp increase beyond that amount suggests near failure conditions at 9% wax and hence greater variability in behavior, as noted. On the other hand, 85% TMD charges show linearity up to 15% wax (see Figure 5b). This result emphasizes the importance of porosity as well as the accompanying increase in explosive concentration. Both the 70% and 85% TMD series show decreasing acceleration of the convective flame front with increasing wax content. In fact, the charge containing 15% wax shows no acceleration or, possibly, a small deceleration (see Table 4). We believe that the pressure and rate of change of the pressure behind the convective front is responsible for the specific acceleration observed. It follows that the increasing wax content must react with the HE in such a way as to change the driving pressure, dp/dt, and the energy per unit volume; these changes are then reflected in the observed changing acceleration of the convective front.

*There is also a 2.8% difference in the % TMD value of the two charges at a steep portion of the ℓ vs % TMD curve.

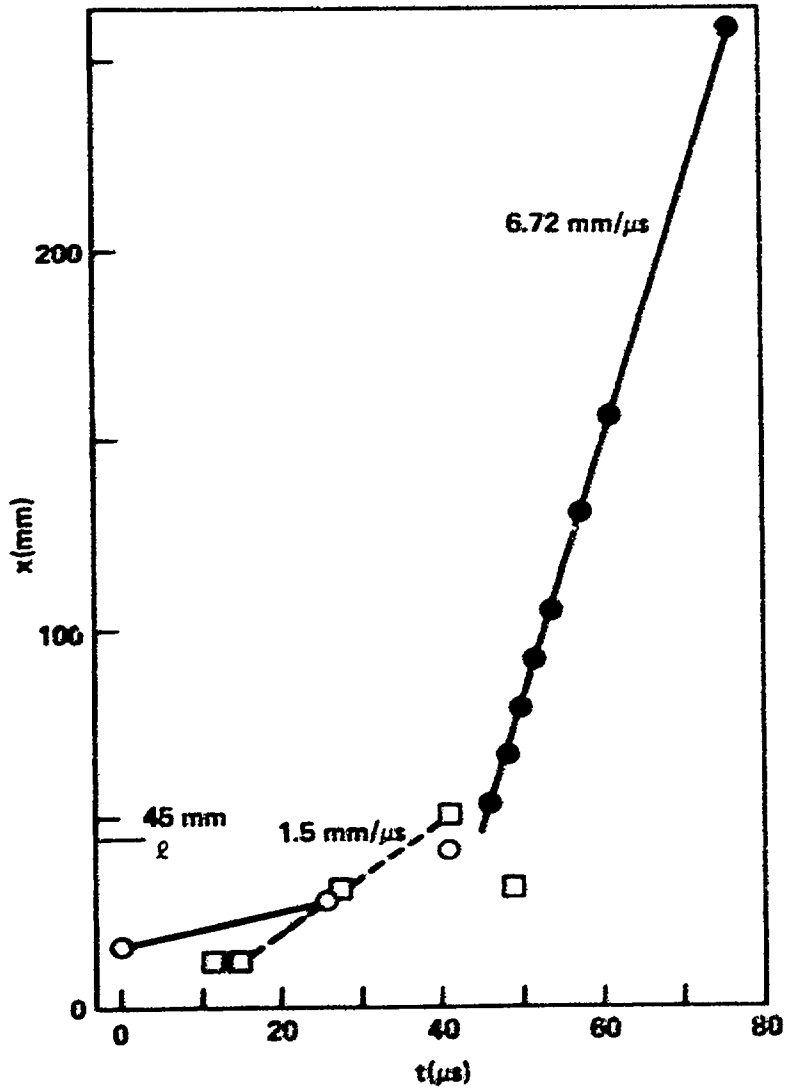

a. DISTANCE-TIME DATA. (○ WOL PROBES, ● COMMERCIAL PROBES, □ SG EXCURSION TIME.)

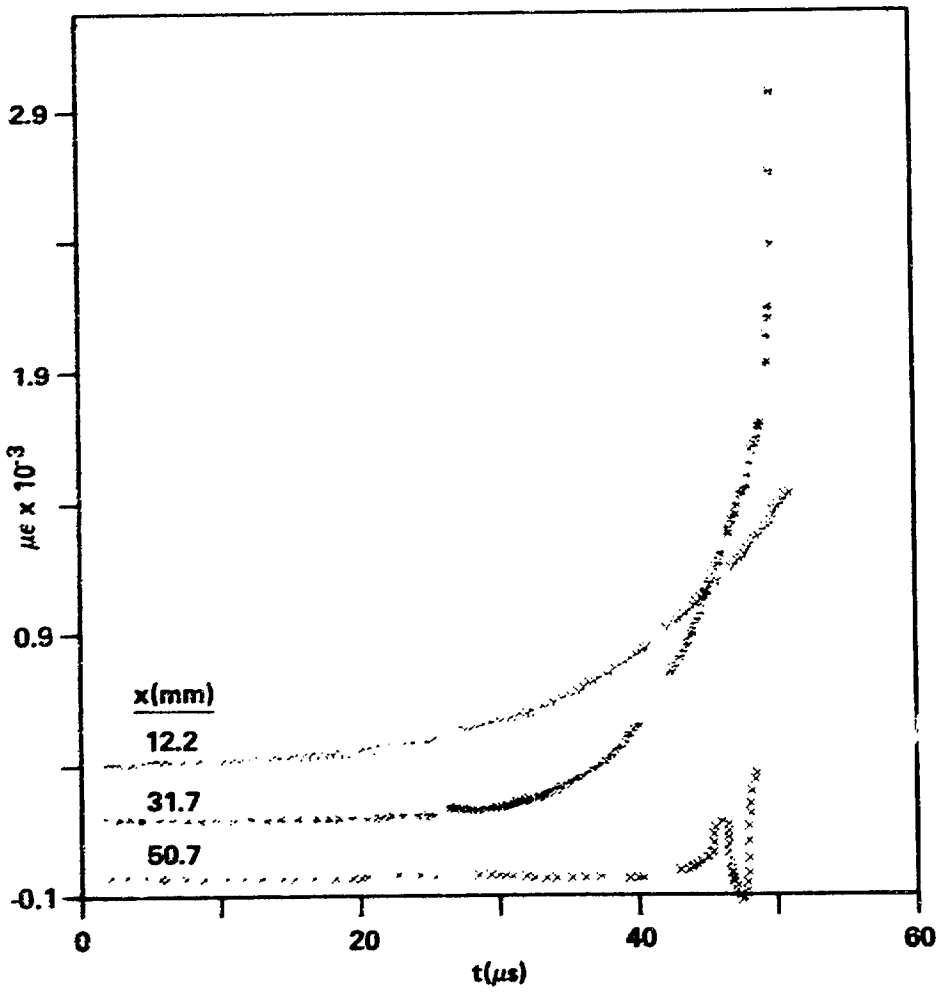

b. STRAIN-TIME DATA. (EACH CURVE, EXCEPT THE LOWEST, HAS BEEN RAISED 200με (OR AN INTEGRAL MULTIPLE THEREOF) FOR BETTER DATA DISPLAY.)

FIG. 4 SHOT 911 ON 69.1% TMD, CLASS A RDX, ρ_o = 1.25 g/cc.

Table 3. Summary of Data for Waxed RDX at 70% TMD

Shot No.	%Wax	ρ_o g/cc	% TMD	B[e] mm/μs	2Cx10^3 mm/μs^2	V_{PC} mm/μs	ℓ mm	$^{41}\Delta t_D$ μs	$^{41}\Delta t_p$ μs	$^{41}\Delta t_E$ μs	Source of data
911	0	1.25	69.1	(≤0.48)	-	1.3-1.5	45	5	<0	-	Table 2; Fig. 4
218	3	1.25	70.9[a]	0.44	3.3	-	95	79	-	-	TR 72-202
214	6	1.21	70.3[b]	0.36	0.82	-	135	182	-	-	TR 72-202
225	9	1.17	69.8[c]	0.26	0.39	1.9	275	610	483	127	TR 72-202
406	0	1.25	69.1	-	-	-	40	0	-	-	Table 2; Fig. C1a
404	3	1.25	70.9[a]	(0.47)	-	∿0.99	72	32.5	1.5	31	Appendix D
401	6	1.21	70.3[b]	0.32	0.55	0.92	130	186	97	89	Table 1; Fig. A1
411	9	1.22	72.6[c]	(0.16)	>0	0.87	∿220	550	410	140	Appendix D
405	12	1.17	71.3[d]	0.25	0.19	-	F	-	-	-	Appendix D

	ρ_v, g/cc
a.	1.76
b.	1.72
c.	1.68
d.	1.64

e. From $x = A + Bt + Ct^2$ with B the value of x = 41 mm; numbers in parentheses are computed from first two (or second and third) IP discharge times.

Table 4. Summary of Data for Waxed RDX at 85% TMD

Shot No.	% Wax	ρ_o	% TMD	B[e] mm/μs	$2C \times 10^3$ mm/μs^2	V_{PC} mm/μs	ℓ mm	$^{41}\Delta t_D$ μs	$^{41}\Delta t_p$ μs	$^{41}\Delta t_E$ μs	Source
–	6	–	85.0[a]	–	–	–	96	51	10.5	40.5	Read from Fig. 1&2
306	9	1.44	85.5[b]	0.54[f]	1.3	1.3	155	149	86	63	TR 72-202
415	12	1.40	85.2[c]	0.37[g]	0.33	1.9	176	208	115	93	Appendix D
505	15	1.36	84.9[d]	0.48	0[h]	1.3	232	342	220	122	Appendix D

	ρ_v, g/cc
a	1.72
b	1.68
c	1.64
d	1.61

e From $x = A + Bt + Ct^2$; B is value at x = 41 mm. Values in parentheses are estimates from first two points.

f In this case, value at x = 28.7 mm; at 41 mm, value is 0.59 mm/μs.

g In this case, value at x = 28.2 mm; at 41 mm, value is 0.38.

h Could be small negative value.

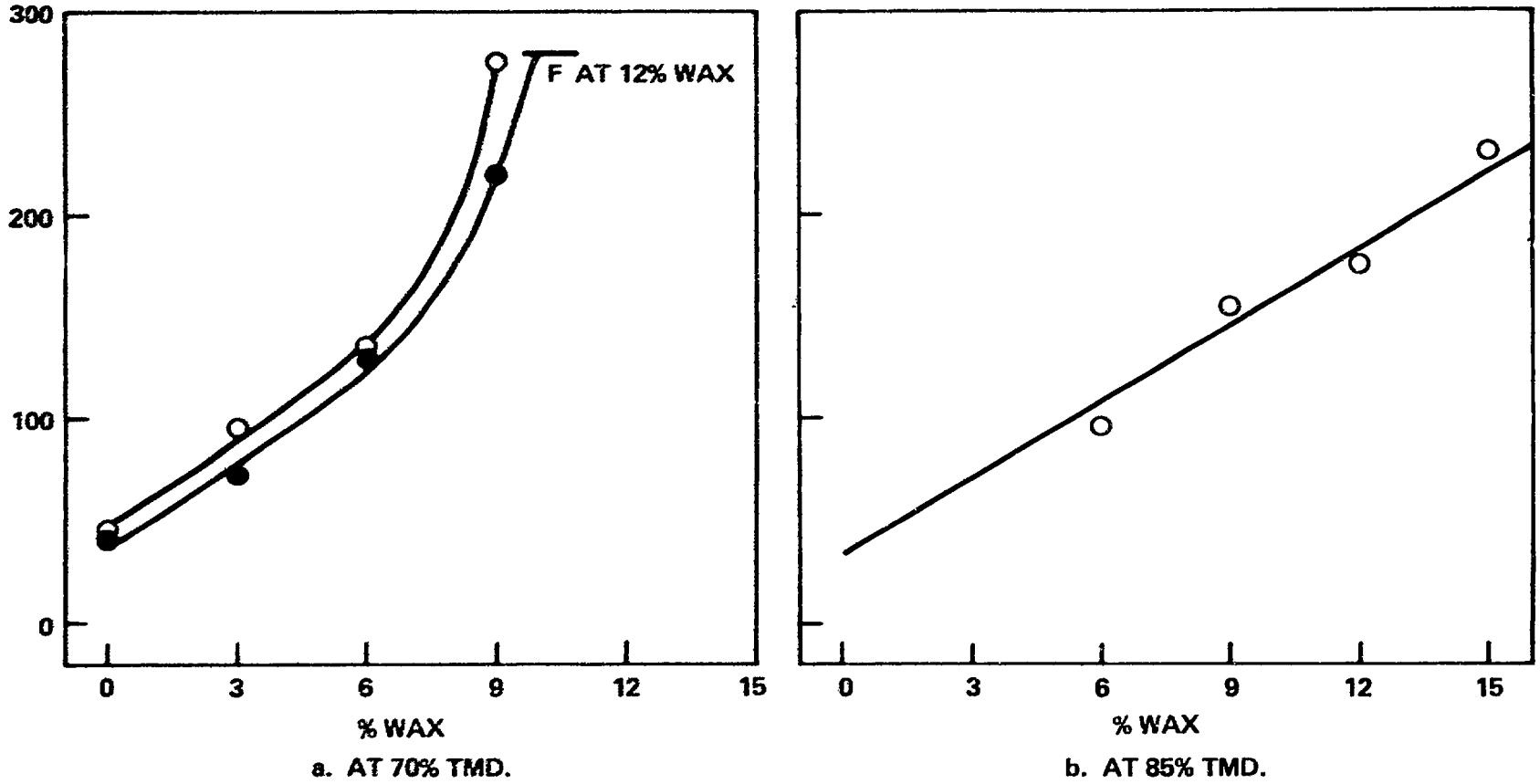

FIG. 5 PREDETONATION COLUMN LENGTH AS FUNCTION OF WAX CONTENT IN RDX/WAX.

Table 5 summarizes the data for two HMX/wax series at 70% TMD; the series were prepared from Class A HMX and a narrow sieve cut ($\bar{\delta} \sim 115\mu$) from the same material. Detailed data and their plots are given in Appendix D. Summary plots of the effect of wax on the two samples of HMX are shown in Figure 6. The waxed HMX (Class A) produced ℓ values very close to those of waxed RDX (Class A). In fact, up to the 9% wax level, the top curve of Figure 6 is a better check for the lower curve of Figure 5 than the replicate run on waxed Class A RDX. At 12% wax, the HMX showed a stronger buildup in pressure sooner than did the RDX/wax (neither showed transition). Both Class A and 115μ HMX show a linear increase of ℓ with % wax only up to 6% wax. At 9% wax, the waxed HMX appears to be approaching critical conditions in the experimental setup used. In other words the Class A HMX gave a waxed series that closely paralleled that of Class A RDX in ℓ values. Moreover, the waxed series of the 115μ HMX paralleled the Class A HMX series though at a somewhat lower value. It seems reasonable to assume that both series will show a linear increase with wax content at 85% TMD and higher compactions.

Up to 6% wax, waxed HMX (Class A) cannot be distinguished, within experimental error, from waxed HMX ($\bar{\delta} \sim 115\mu$) by the ℓ values, but at higher concentrations the two series can be distinguished both by ℓ values and the characteristics of the SG records, as shown in Table 6. Moreover, the fact that the waxed Class A ($\sim 200\mu$) HMX showed a greater predetonation column length ℓ than did the narrow sieve cut (115μ) is of particular interest because it is the reverse of the usual and reported trend of increased ℓ with decreased particle size. In fact it is the reverse of our own results on pure and waxed RDX (above) and on fine and coarse tetryl (4). Presumably the reversal was caused by removal of the fines, but this will have to be checked.

Because of unexpected effects (such as the above) caused by the specific range of particle size in the explosive, it is the preferred experimental practice to work with narrow screen cuts, i.e., a relatively small range in particle size. However, we found in obtaining the 115μ HMX, that sieving Class A is too lengthy and too expensive to be practical.

Table 6 contains some of the results from analyses of the strain gage records. In general, they reinforce the conclusions reached by considering ℓ: HMX(A) is very similar to RDX(A) in wax mixtures; it may have a slightly greater tendency to undergo transition in DDT, but the present data are insufficient to show a significant difference. HMX (115μ) does show a greater tendency to transit than either of the Class A materials.

4. D. Price, R. R. Bernecker, J. O. Erkman, and A. R. Clairmont, Jr., "DDT Behavior of Tetryl and Picric Acid," NSWC/WOL/TR 76-31, 21 May 1976.

Table 5. Summary of Data for Waxed HMX at 70% TMD

Shot No.	% Wax	ρ_o g/cc	% TMD	b[f] mm/μs	V_{PC} mm/μs	ℓ mm	$^{41}\Delta t_D$ μs	$^{41}\Delta t_p$ μs	$^{41}\Delta t_E$ μs
				$\bar{\delta} \sim 115\mu$					
1605	0	1.32	69.4[a]	0.9	-	35	0	-	?
1610	3	1.31	70.7[b]	0.51	1.14	67	22	0	22
1608	6	1.27	70.4[c]	0.38	1.06	99	87	31	56
1611	9	1.23	69.9[d]	0.38	0.7	143	197	80	117
1615	12	1.19	69.3[e]	0.47	0.7	273	~569	~255	314
				$\bar{\delta} \sim 200\mu$ (Class A)					
1616	0	1.32	69.4	0.43	~1.3	45	1.7	1.2	0.5
1617	6	1.27	70.4	0.23	0.8	119	144	63	81
1618	9	1.23	69.9	0.23	1.1	210	395	216	179
1701	12	1.19	69.3	0.27	0.8	F	F	F	F

a ρ_v = 1.902 g/cc

b ρ_v = 1.852

c ρ_v = 1.804

d ρ_v = 1.759

e ρ_v = 1.716

f Slope given by data of first two IPs; all curves showed acceleration except Shot 1615 where curve was linear.

Detailed data for these shots appear in Appendix D.

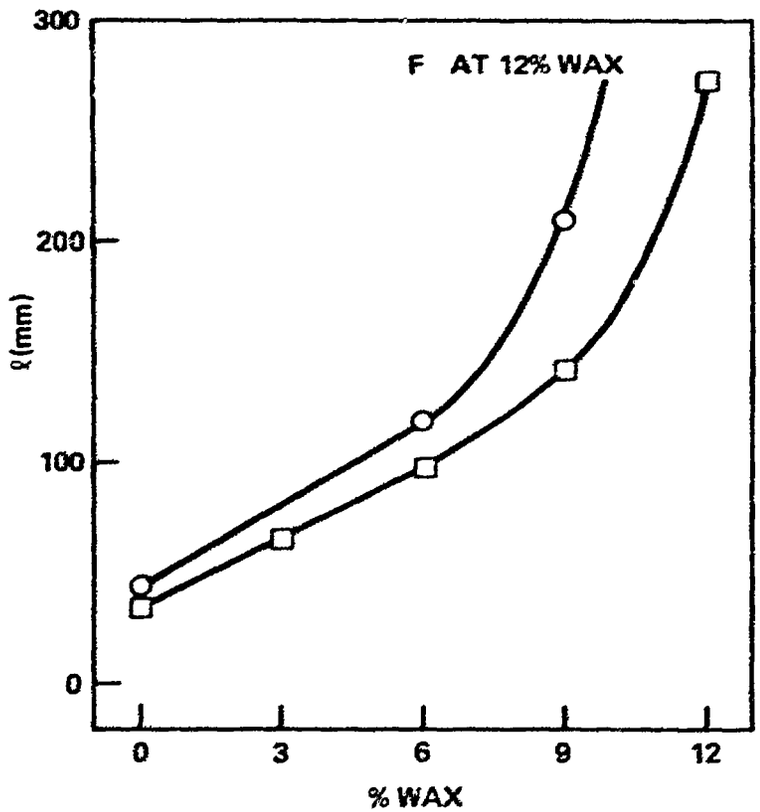

FIG. 6. PREDETONATION COLUMN LENGTH AS A FUNCTION OF WAX CONTENT IN HMX/WAX AT 70% TMD, (○ HMX 900, CLASS A; □ 115μ SCREEN CUT FROM SAME HMX).

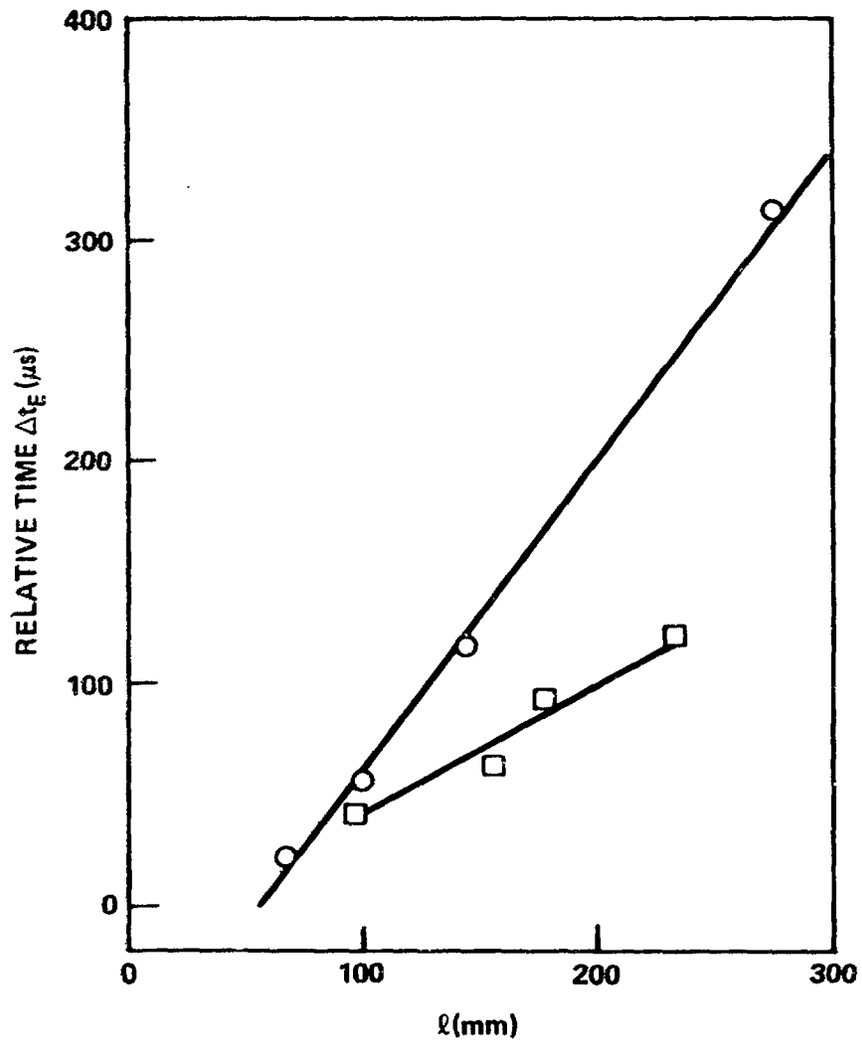

FIG. 7. RELATION Δt_E VS ℓ FOR WAXED HE, (○ HMX SERIES AT 70% TMD; □ RDX SERIES AT 85% TMD).

Table 6. Details from Records of Some Shots at 70% TMD
(See Appendices A & D)

Shot Number	Fig.	HE	Velocity of Convective Front mm/μs	PC Front Velocity mm/μs	PC Front Time at x = 41 mm	No. of SG Records Indicating Possible Shock Formation*
			94/6 HE/Wax			
401	A1	RDX(A)	0.3	0.9	80	None
1617	D12	HMX(A)	0.2	0.9	95	None
1608	D8	HMX(115μ)	0.5	1.1	60	None
			91/9 HE/Wax			
411	D2	RDX(A)	0.2	0.9	500	One
1618	D13	HMX(A)	0.2	1.1	250	One
1611	D9	HMX(115μ)	0.4	0.7	100	Three
			88/12 HE/Wax			
405	D3	RDX(A)	0.3	---	900-1000**	One
1701	D14	HMX(A)	0.3	0.8	525	One
1615	D10	HMX(115μ)	0.5	0.7	375	Three

* Sharp dip, negative $(\frac{dp}{dt})$; only SGs with x<ℓ considered.

**Estimated from one good SG record at x = 118 mm.

Of the 6 - 9% waxed HMX shots (both Class A and 115μ particle size) all four shots gave data showing a transition behavior clearly that proposed initially for 91/9 RDX/wax and subsequently applied to pure HE as well. The 0 - 3% waxed HMX shots produced less complete data but were consistent with the original mechanism.

Among the parameters tabulated in the summary Table 5 are relative times (defined in Table 1). It is of considerable interest that there seems to be a strong correlation between Δt_D and ℓ, and Δt_E and ℓ; the latter is linear. This relationship is evident at a constant % TMD and varying wax content, as illustrated in Figure 7 for waxed HMX (115μ) at 70% TMD and for waxed RDX(A) at 85% TMD. It is of equal interest that no similar correlation appears at fixed composition and varying % TMD, e.g., 94/6 RDX/wax of this report and 91/9 RDX/wax of reference 1. However, an analogous correlation (only the Δt_E vs ℓ) appears for several gas loaded explosives at 70(or 88)% TMD (5) where the variation of composition is that shown by different pure organic HE.

E. Waxed Tetryl

Data for two shots on waxed tetryl are given in Appendix E. One confirms the previously reported mechanism for 97/3 tetryl/wax (4); the other shows a failure of 91/9 tetryl/wax to undergo DDT.

IV. SUMMARY AND CONCLUSIONS

1. The 94/6 RDX/wax series gave DDT data showing trends quite similar to the 91/9 series with the time ranges for all effects shortened. In particular, there is a trend for variation of Δt_D (relative time to detonation with zero time at first IP, x = 41 mm) and of Δt_E (relative time to detonation after formation of PC wave) with % TMD.

2. 91/9 RDX/wax exhibits DDT in our apparatus at as high a compaction (97%) as could be obtained with the hydraulic press.

3. Pure RDX exhibits the same mechanism proposed for 91/9 RDX/wax (1). This is also true for all the waxed mixtures of this report.

4. Class A RDX and HMX are indistinguishable (in our apparatus) in their DDT behavior. So too are their waxed series.

5. D. Price and R. R. Bernecker, "Method Used to Assess Sensitivity to DDT of Shell Fills", paper for Conference on the Standardization of Safety and Performance Tests for Energetic Materials, ARRADCOM Dover, New Jersey, June 1977.

5. A narrow sieve cut of HMX ($\bar{\delta}$ ~ 115μ), made from Class A HMX ($\bar{\delta}$ ~ 200μ), used in a waxed series, showed smaller ℓ values than the corresponding Class A mixtures. This reversed the apparent particle size effect found in two other comparisons: pure RDX and waxed RDX. For these last, the smaller $\bar{\delta}$, the larger ℓ.

6. Correlations between ℓ and Δt_D and between ℓ and Δt_E are evident for the waxed series at constant porosity (waxed HMX at 70% TMD and waxed RDX at 85% TMD). These relations seem reasonable in that burning rate and reactivity should decrease with increasing wax content.

7. No similar correlation between ℓ and Δt_D or Δt_E is evident at fixed composition, initial particle size, and % TMD. Presumeably, change in permeability has more complex effects on DDT than simple dilution with wax.

VI. REFERENCES

1. R. R. Bernecker and D. Price, "Transition from Deflagration to Detonation in Granular Explosives", NOLTR 72-202, 13 Dec 1972.
2. R. R. Bernecker and D. Price, "Sensitivity of Explosives to Transition from Deflagration to Detonation", NOLTR 74-186, 7 Feb 1975.
3. J. Calzia, "Experiments on the Deflagration-Detonation Transition in Condensed Explosives," Compt Rendu 276, 1397-99, (1973).
4. D. Price, R. R. Bernecker, J. O. Erkman, and A. R. Clairmont, Jr., "DDT Behavior of Tetryl and Picric Acid," NSWC/WOL/TR 76-31, 21 May 1976.
5. D. Price and R. R. Bernecker, "Method Used to Assess Sensitivity to DDT of Shell Fills", paper for Conference on the Standardization of Safety and Performance Tests for Energetic Materials, ARRADCOM Dover, New Jersey, June 1977.

APPENDIX A

Detailed Data for 94/6 RDX/Wax Series

The distance-time (x-t) data for this series of shots appear in Table A1. They are plotted as two part figures in order of increasing compaction. In each case, part (a) displays x-t data; part (b), strain-time data. As in earlier work, open circles indicate discharge time and position of the custom-made probes; solid circles, those of commercial probes. Squares are used to show position and time of rapid pressure rise, as indicated by the strain gage (SG) records. Numbers on the SG curves indicate location of the SG given as x in mm.

The interpretation and analysis is straightforward, and in most cases, analogous to similar data in reference 1. An exception occurs in Shot 801, however. Here ℓ cannot be determined from tube fragments and the discharge time of the IP at 105 mm is out of line with those of the later probes showing steady state detonation. It so happened that a SG was also at about 105 mm; its record (Figure A5b) shows the familiar negative slope associated with shock or shock formation just prior to discharge of the ionization pin at 105 mm. Consequently an ℓ value just beyond this region was chosen, i.e. $\ell = 110 \pm 5$ mm places the onset beyond the shock disturbance region and on the extrapolated x-t curve for steady state detonation.

In this same shot, an extended (in time) record was recorded for the SG at 20.3 mm. It recorded a very high strain level (6000 $\mu\varepsilon$) and maintained it for about 70 μs although detonation began (at x = 110 mm) at 36.3 μs on the same time scale.

As might be expected, the records of the 94/6 RDX/wax series indicate the same mechanism of DDT as the physical model proposed for the 91/9 RDX/wax series(1).

Table A1. Compilation of Distance-Time Data for 94/6 RDX/Wax Experiments

Shot No.	914[c]			801[b]		717[b]	
Density g/cc:	1.664			1.62_9		1.55_3	
% TMD[a]	96.8			94.7		90.3	
Ionization Probe Data	x	t		x	t	x	t
	41.5	0.0*	Double	28.7	0.0*	28.7	0.0*
		1.39	discharge	41.4	5.8*	41.4	12.3*
	60.6	16.06*		54.1	13.2*	54.1	21.9*
	79.6	27.21*		79.5	26.85	66.8	30.5
	105.0	38.38		104.9	36.1	79.5	38.0
	124.1	44.19		130.4	38.75	104.9	40.9
	143.1	46.52		155.8	41.7	130.3	44.0
	162.2	48.45		181.2	44.8	155.8	47.4
	181.2	50.79		206.6	47.55	206.6	53.5
	206.6	53.94		257.3	53.85	257.4	60.2
	232.2	56.92					
	257.6	60.17					
Strain Gage Data	x	t_{PC}		x	t_{PC}	x	t_{PC}
	20.8	–		20.3	–	20.8	–
	60.8	21.8		47.9	11±2	47.8	16^{-1}_{+0}
	80.0	29.1		66.8	18.5	67.0	24.5
	99.1	33.7		86.1	28.0	86.1	35.0
	118.0	40.4 (destroyed at 43.2).		105.3	33.5	105.2	–
ℓ, mm	114^{+5}_{-0}			110±5		95^{+5}_{-0}	
D, mm/μs	8.38			8.42		7.92	
σ, mm/μs	0.09			0.10		0.08	

a ρ_v = 1.72 g/cc, b 1215 Steel tube (bar), c 1018 Steel tube (bar), d 1018 Steel tube, *Custom-made probes

Table A1. (CONT)
Compilation of Distance - Time Data for 94/6 RDX/Wax Experiments

Shot No.	703[c]		502[d]		401[d]	
Density g/cc:	1.51_0		1.40_2		1.21_0	
% TMD[a]	87.8		81.5		70.3	
Ionization Probe Data	x	t	x	t	x	t
	28.7	0.0*	23.1	0.0*	41.4	0.0*
	41.4	13.4*	34.7	24.7*	66.8	74.1*
	54.1	22.6*	47.6	52.6	92.2	140.7
	66.8	35.55*	60.45	78.6	104.9	167.2
	79.5	44.2	79.5	107.65	117.6	-
	104.9	51.05	92.2	117.0	130.3	185.6
	130.3	54.0	104.9	119.1	168.4	191.65
	155.7	57.6	117.6	121.1	193.8	195.9
	206.5	63.5	155.7	126.1	219.2	199.7
	257.3	70.2	256.8	139.9	263.65	207.0
Strain Gage Data	x	t_{PC}	x	t_{PC}	x	t_{PC}
	20.4	-	20.7	38,47	29.0	86,118
	41.8	13	42.2	64	53.9	110
	60.5	28	66.9	86,90	79.5	142
	79.9	40	117.6	-		
	98.5	46.5				
ℓ, mm	105^{-0}_{+5}		92^{-5}_{+0}		130 ± 5	
D, mm/μs	7.97		7.26		6.24	
σ, mm/μs	0.12		0.10		0.04	

a ρ_v = 1.72 g/cc
b 1215 Steel tube (bar)
c 1018 Steel tube (bar)
d 1018 Steel tube (tube)
*Custom-made probes

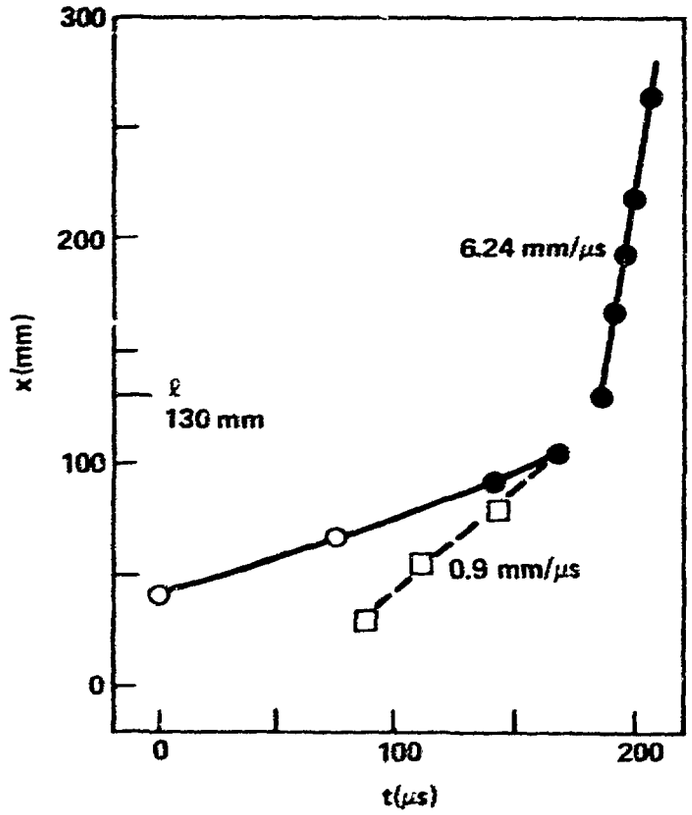

a. DISTANCE-TIME DATA (USE KEY OF FIGURE 4a).

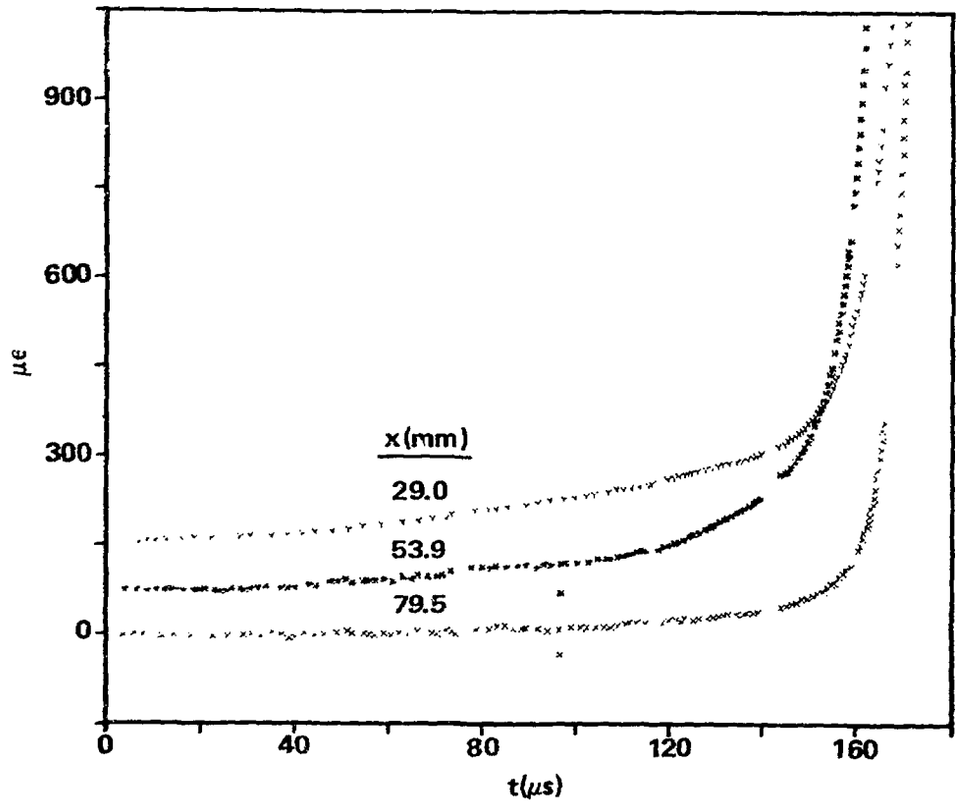

b. STRAIN-TIME DATA (KEY OF FIGURE 4b WITH INCREMENT 75$\mu\epsilon$).

FIG. A1. SHOT 401 ON 70.3% TMD 94/6 RDX/WAX, ρ_o = 1.21 g/cc.

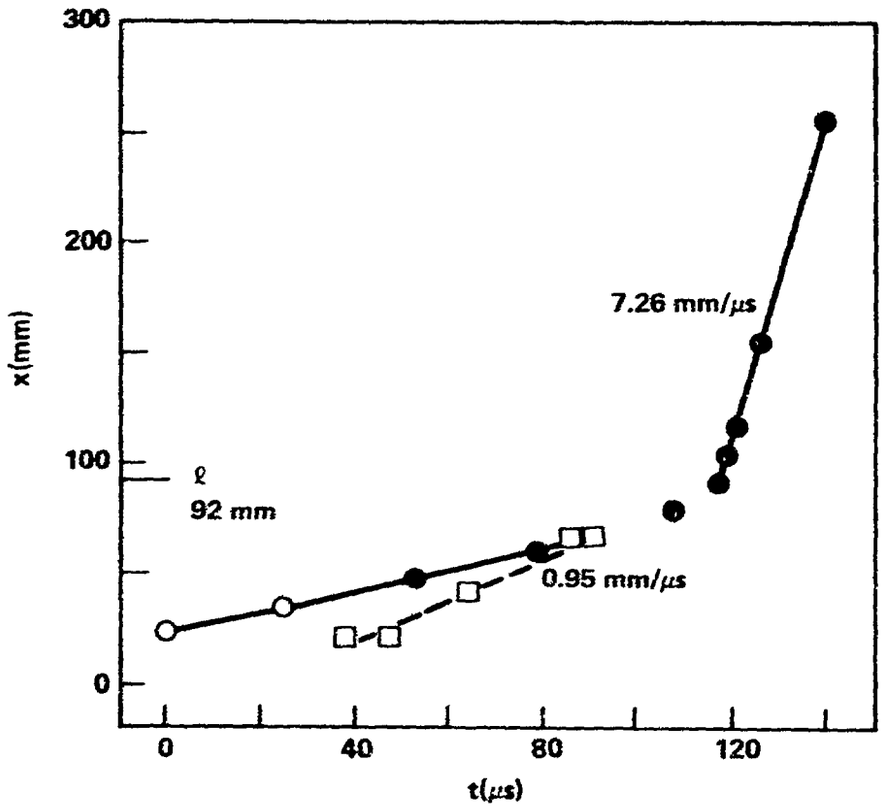

a. DISTANCE-TIME DATA (KEY OF FIGURE 4a).

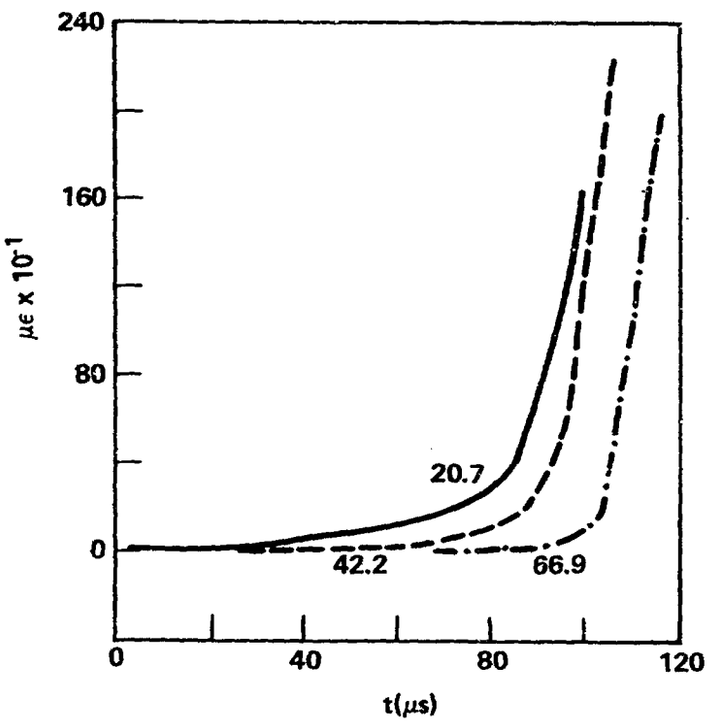

b. STRAIN-TIME DATA.

FIG. A2. SHOT 502 ON 81.5% TMD 94/6 RDX/WAX, ρ_o = 1.40 g/cc.

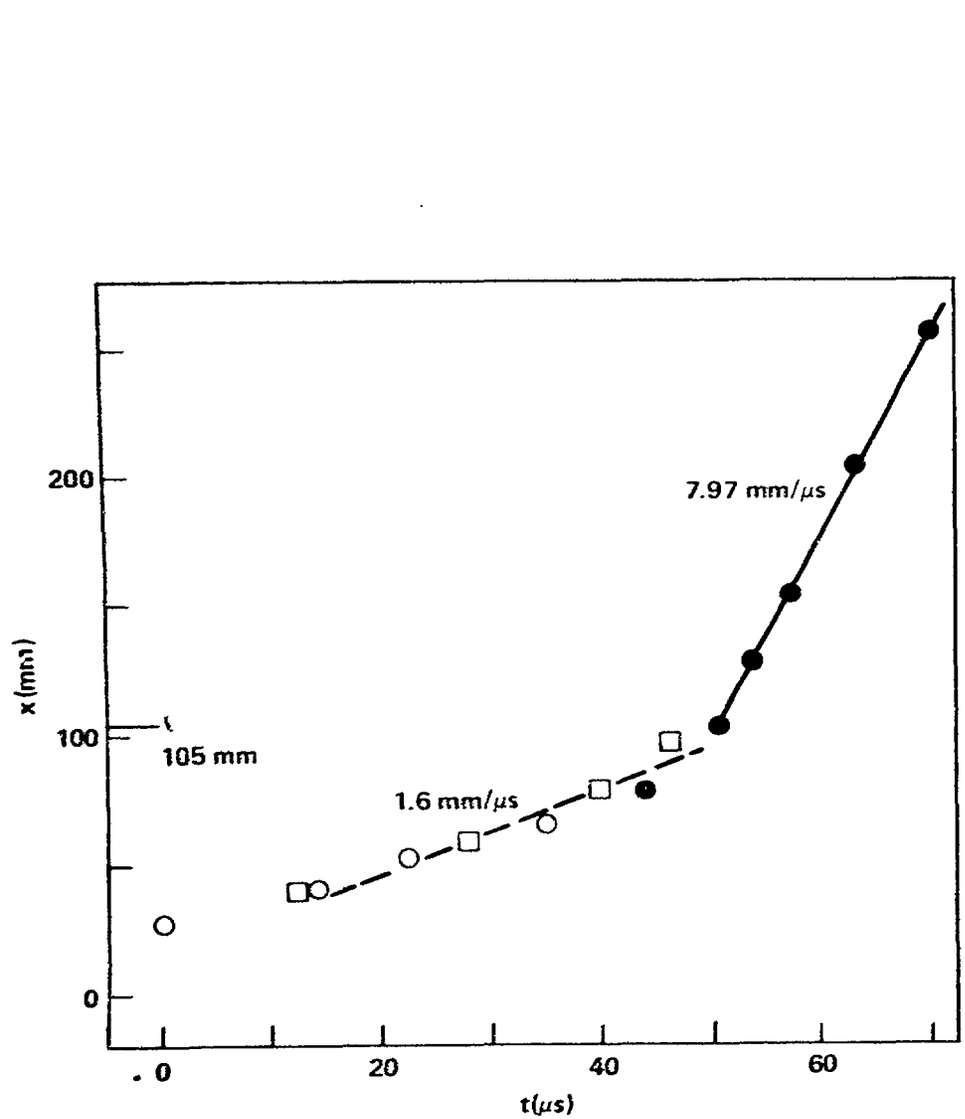

a. DISTANCE-TIME DATA (KEY OF FIGURE 4a).

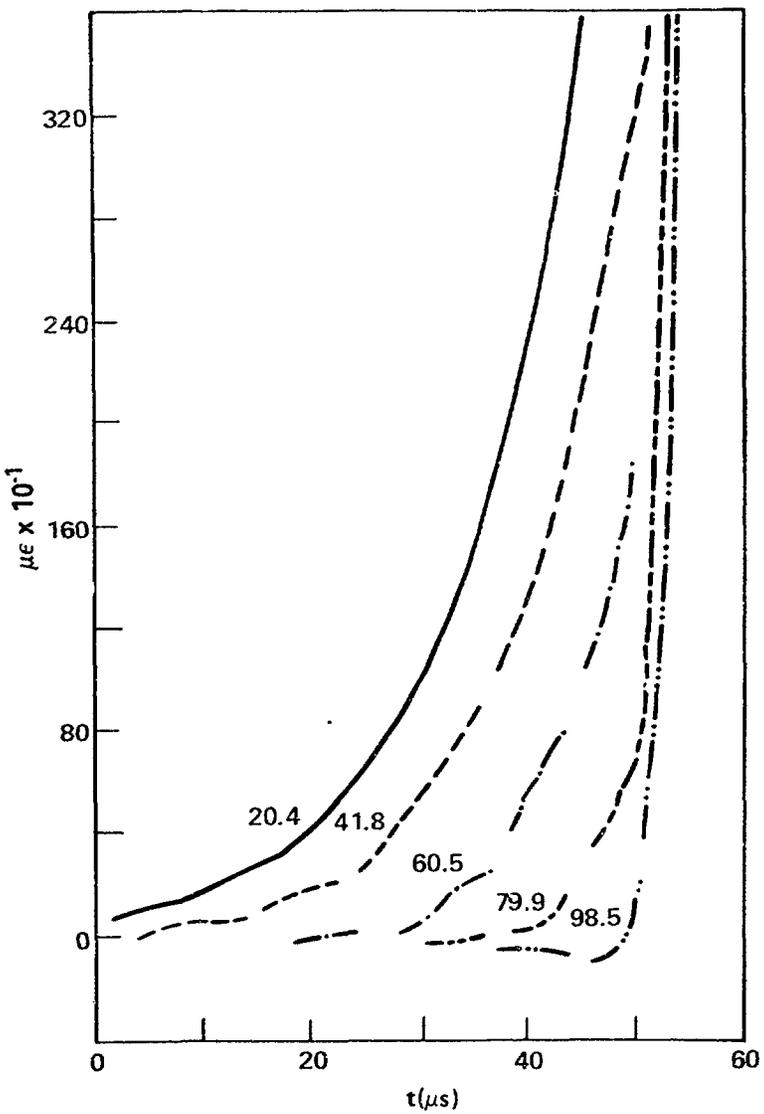

b. STRAIN-TIME DATA.

FIG. A3. SHOT 703 ON 87.8% TMD 94/6 RDX/WAX; ρ_o = 1.51 g/cc.

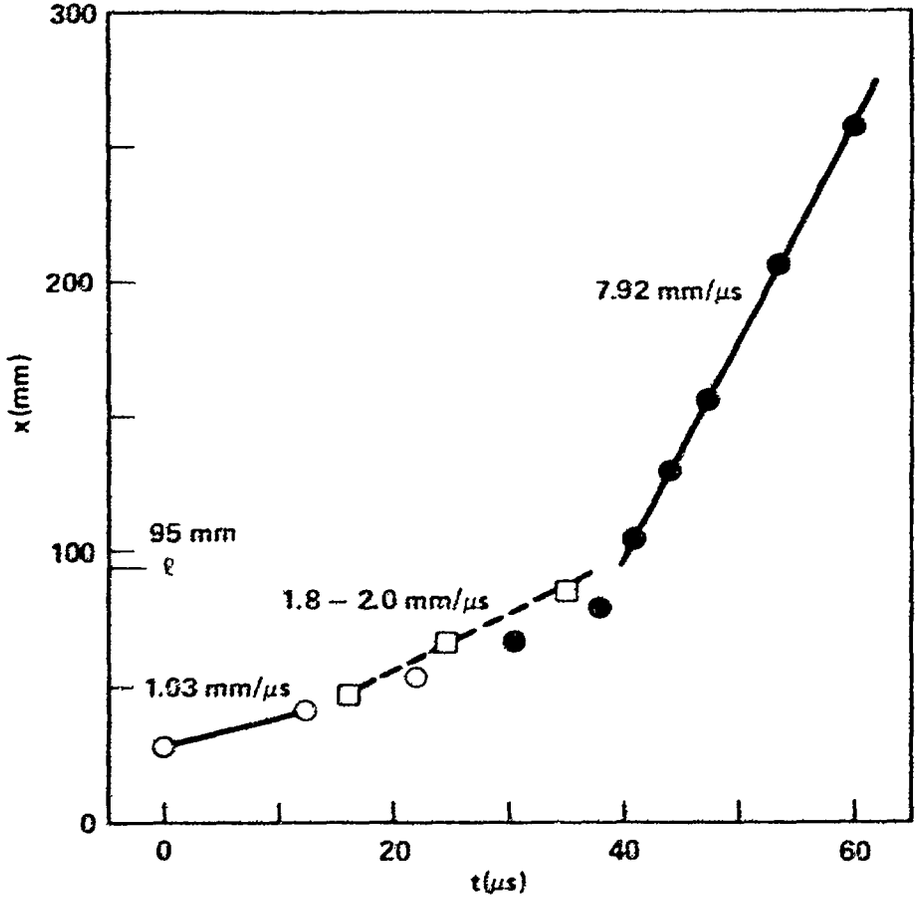

a. DISTANCE-TIME DATA (KEY OF FIGURE 4a).

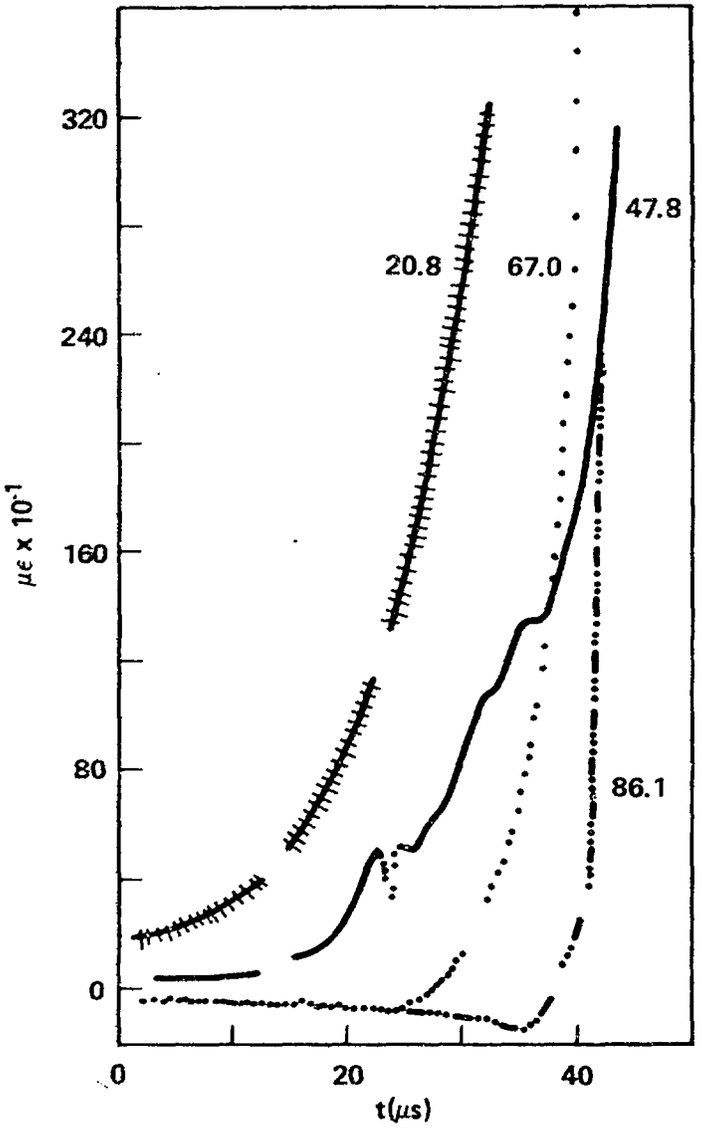

b. STRAIN-TIME DATA.

FIG. A4. SHOT 717 ON 90.3% TMD 94/6 RDX/WAX, ρ_o = 1.55 g/cc.

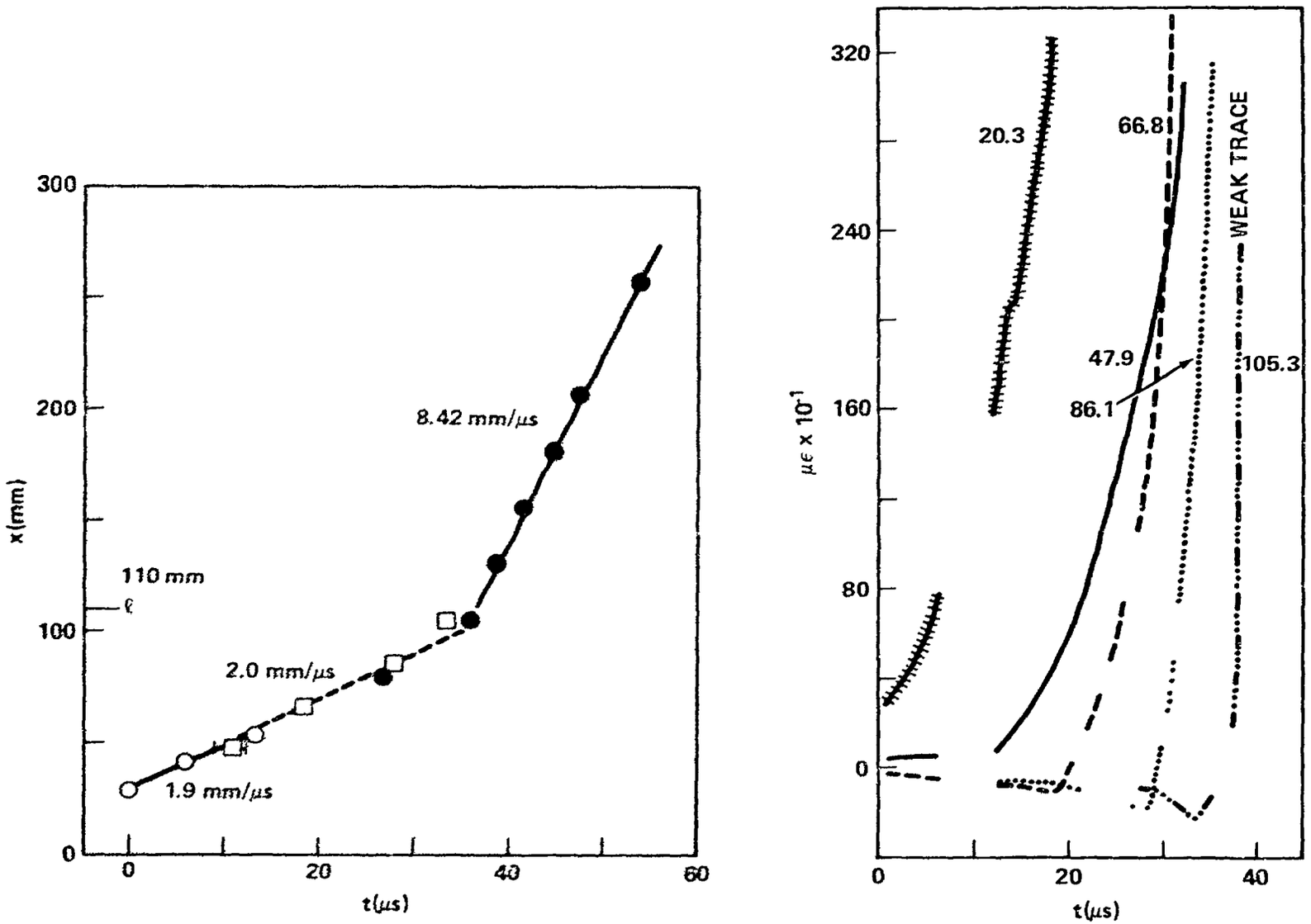

a. DISTANCE-TIME DATA (KEY OF FIGURE 4a).

b. STRAIN-TIME DATA.

FIG. A5. SHOT 801 ON 94.7% TMD 94/6 RDX/WAX, ρ_o = 1.63 g/cc.

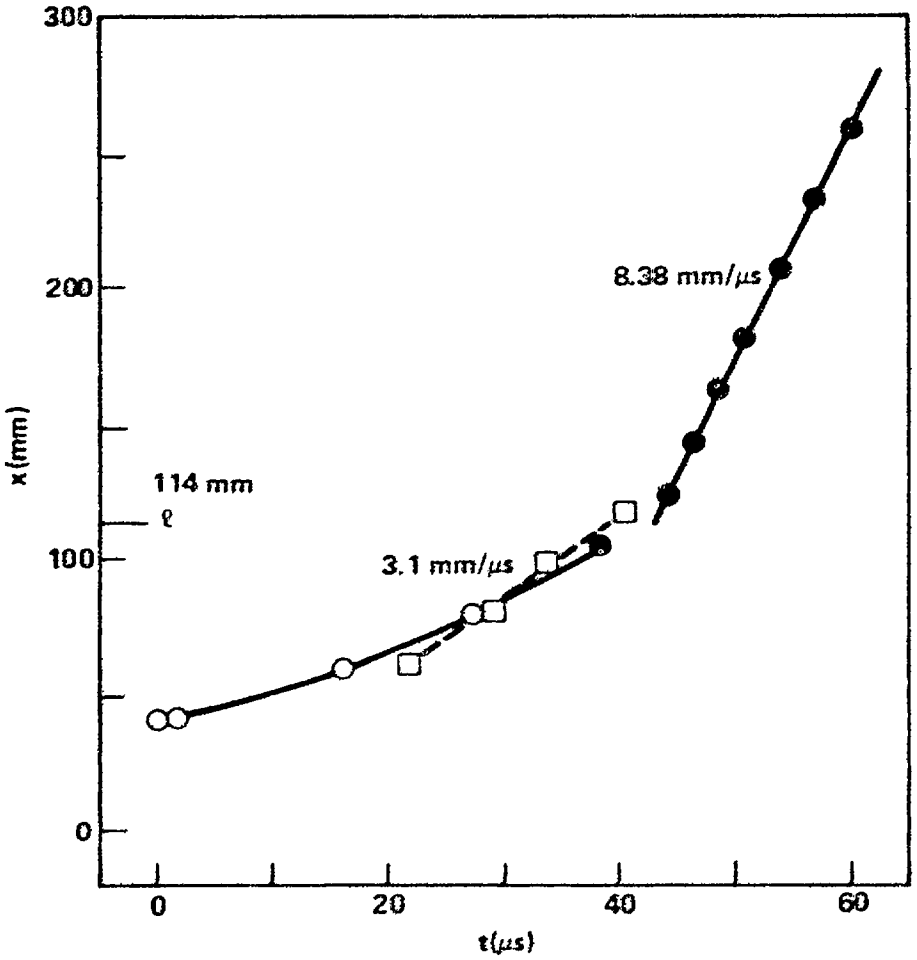

a. DISTANCE-TIME DATA (KEY OF FIGURE 4a).

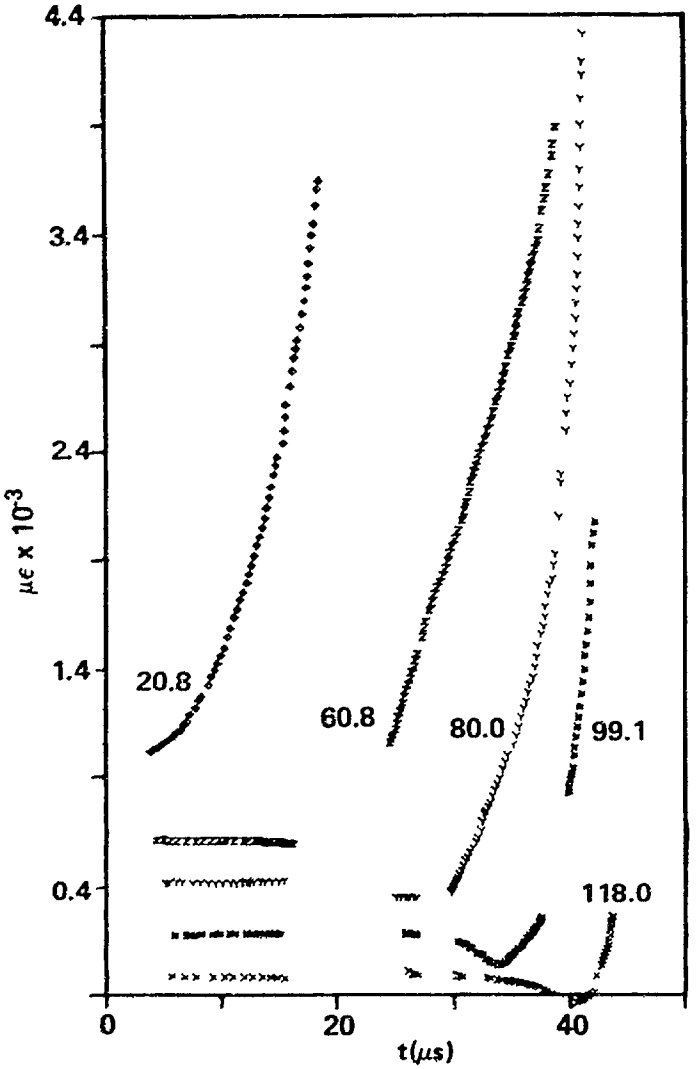

b. STRAIN-TIME DATA (KEY OF FIGURE 4b).

FIG. A6. SHOT 914 ON 96.8% TMD 94/6 RDX/WAX, ρ_o = 1.66 g/cc.

APPENDIX B

Data for 91/9 RDX/Wax Shots

Numerical data appear in Table B1. They are plotted in Figure 3 of the text and Figure B1 for the coarse RDX mixture, and in Figure B2 for the regular RDX mixture.

Figure B2b is a good illustration of the effect of shock formation on SG records. However, interactions of IP discharges have eliminated portions of these records. Hence better illustrations are given in Appendix D.

Table B1. Detailed Data for 91/9 RDX/Wax Shots

Shot No.	603[b]		913[c]	
Density				
g/cc	1.365		1.63	
% TMD[a]	81.3		97.0	
IP Data	x	t	x	t
	41.40	0.00*	41.5	0.0
	54.10	36.22*	60.6	11.75
	79.50	82.71	79.6	25.21
	105.03	113.49	105.0	41.21
	130.43	131.70	124.1	52.03
	155.83	136.73	143.1	60.36
	181.23	139.80	162.2	63.16
	206.63	143.81	181.2	65.42
	232.15	147.24	206.6	68.60
	257.55	150.45	232.2	71.78
			257.6	74.97
SG Data	x	t_{pc}	x	t_{pc}
	20.19	--	20.7	--
	41.65	53.0	79.9	29.8
	67.05	68.0	105.2	40.3
	92.71	87.0	130.8	49.0
			156.0	58.7
B, mm/μs	0.222			
$2Gx10^3$, mm/μs^2	5.891			
D, mm/μs	7.28		~8.1	
σ, mm/μs	0.17			

a ρ_v = 1.68
b Class D RDX
c Class A RDX

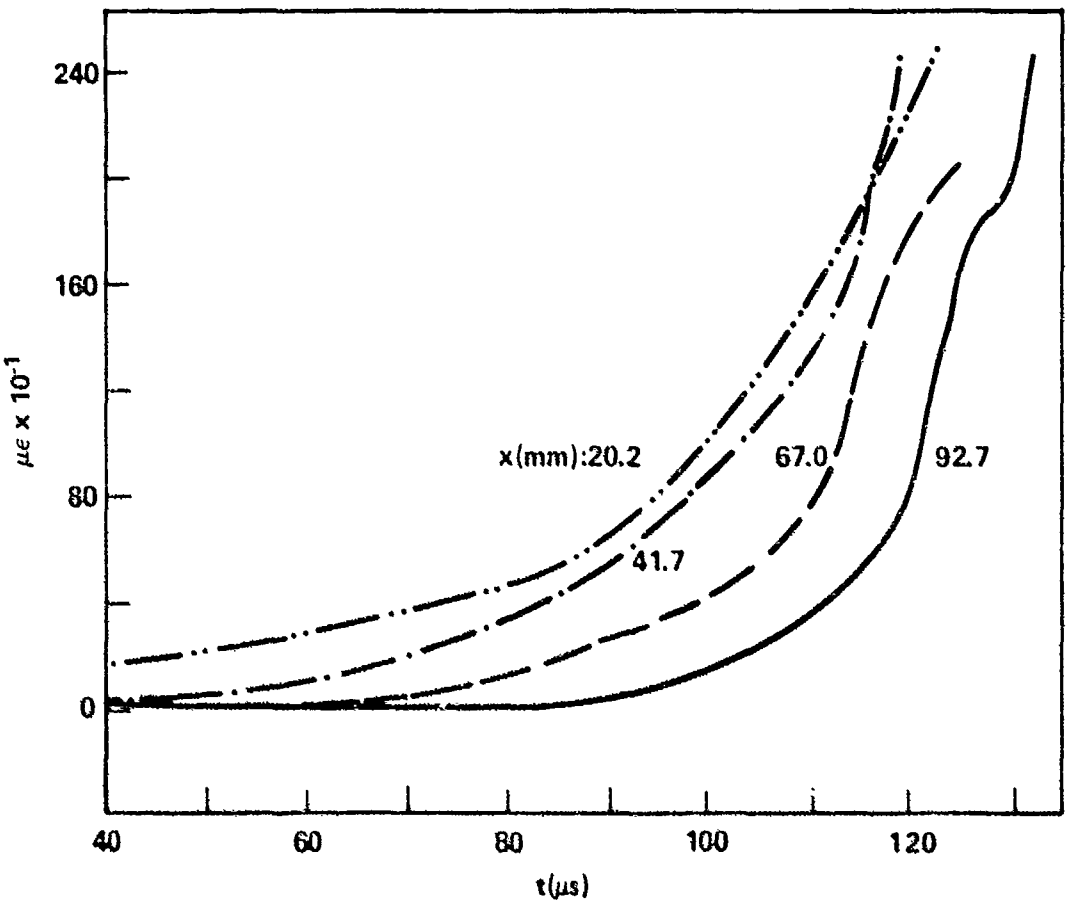

FIG. B1. SHOT 603 ON 81.3% TMD 91/9 RDX (850μ)/WAX, ρ_o = 1.37 g/cc, STRAIN-TIME DATA.

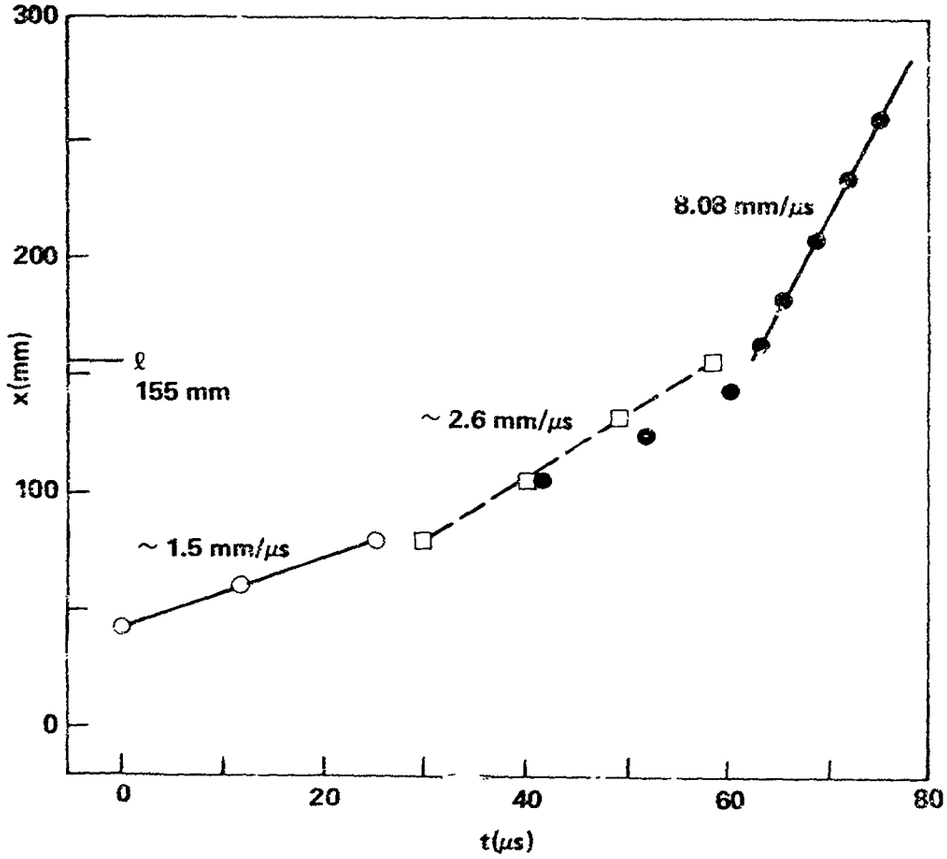

a. DISTANCE-TIME DATA (KEY OF FIGURE 4a).

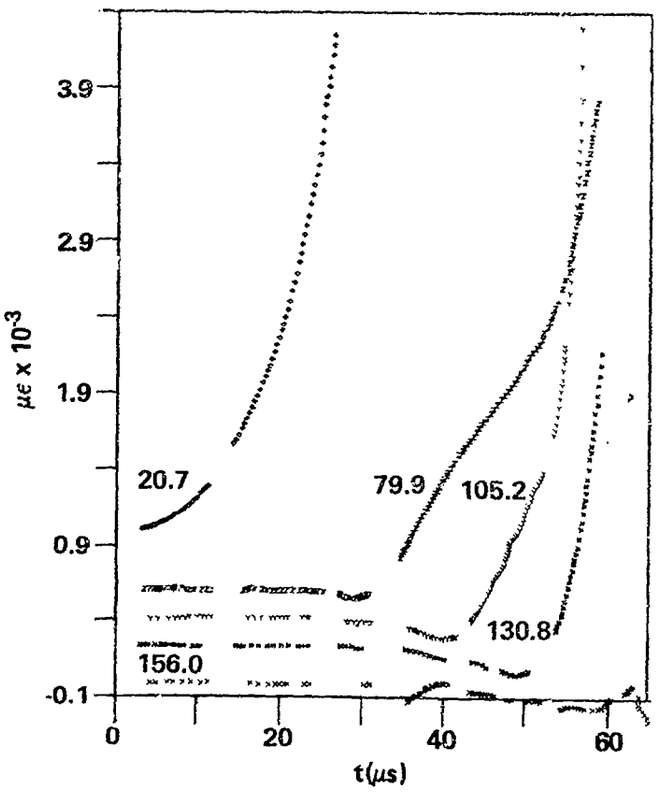

b. STRAIN-TIME DATA (KEY OF FIGURE 4b).

FIG. B2. SHOT 913 ON 97.0% TMD 91/9 RDX/WAX, ρ_o = 1.63.

APPENDIX C

DDT Data for 69.1% TMD RDX, Classes A & E

Data for the four RDX charges are given in Table C1. The space-time plots for Shots 406 and 704 (Class A and Class E RDX, respectively) are shown in Figures C1 and C2. The strain-time records on these shots were short and comparatively uniformative; they have not been reproduced.

Figure C3 displays plots of both IP and SG records for Shot 910, the fine RDX. The space-time plot is of interest in showing a compressive disturbance travelling rearward from the location of the onset of detonation. Since its rate is about that of the forward moving detonation, retonation seems a possibility. However, tube fragments at the igniter end of the tube from this shot were not reported as particularly small nor was a dent in the ignitor bolt noted. For the Class A RDX (Figure 4 of text) only one point of a possible rearward disturbance was found on the SG records, but tube fragments were definitely smaller than usual and the igniter sleeve was crushed.

Table C1. Compilation of Distance-Time Data for RDX

Shot No.	704	406	911	910
Av. Part. Size, μ	∿15	∿200	∿200	∿15
X number	846 (Old 659)	597	597	846
Density g/cc	1.24_8	1.24_8	1.248	1.248
% TMD[a]	69.1	69.1	69.1	69.1
IP Data	x / t	x / t	x / t	x / t
	28.7 / 0.0*	16.3 / 0.0*	16.1 / 0.0*	28.4 / 0.0*
	41.4 / 13.2*	28.8 / 17.85*	28.4 / 25.55*	41.1 / 13.05*
	54.1 / 29.8	41.4 / 22.1	41.4 / 40.75*	53.8 / 23.65*
	66.8 / 30.85	54.1 / 24.0	53.8 / 45.95	66.5 / 25.5
	79.5 / 32.75	66.8 / 26.3	66.5 / 48.25	79.2 / 27.85
	92.2 / 34.5	79.5 / 28.05	79.2 / 49.9	91.9 / 29.6
	104.9 / 36.2	104.9 / 31.75	91.9 / 51.65	104.6 / 31.25
	130.3 / 40.2	155.8 / 39.4	104.6 / 53.75	130.0 / 35.2
	155.7 / 43.95	206.5 / 46.8	130.2 / 57.35	155.4 / 38.7
	257.3 / 59.45	257.3 / 54.4	155.6 / 61.15	257.3 / 53.35
			257.2 / 76.4	
SG Data	x / t_{PC}	x / t_{PC}	x / t_{PC}	x / t_{PC}
Data	20.3 / 6.0?	22.7 / -	12.2 / 11.5-15.0	11.9 / -
	41.4 / -	48.0 / 24.5?	31.7 / 27.5,49.0	31.4 / 7.0,19.0,26.3
	60.2 / -	73.4 / -	50.7 / 41.0	50.3 / 19.5,25.0
	79.7 / -		69.8 / -	69.2 / 25.5, -
	98.5 / -			
ℓ(mm)	60±5	40±5	45±2	55±2
D(mm/μs)	6.65	6.71	6.72	6.88
σ(mm/μs)	0.04	0.03	0.04	0.06

a ρ_v = 1.806 g/cc
* Custom-made probe

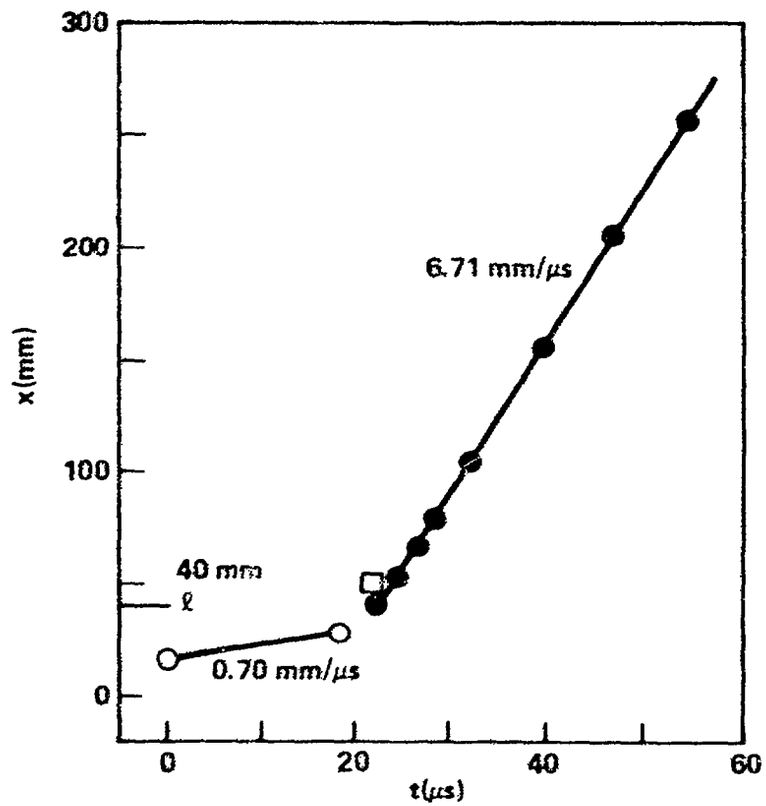

FIG. C1. SHOT 406 ON 69.1% CLASS A RDX, ρ_o = 1.25 g/cc, DISTANCE-TIME DATA (KEY OF FIGURE 4a).

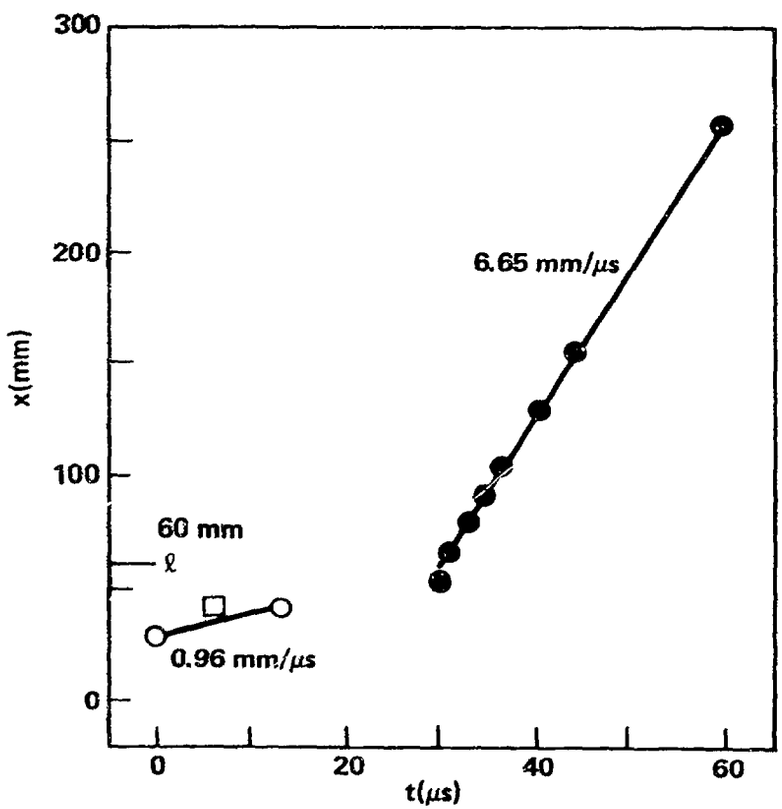

FIG. C2. SHOT 704 ON 69.1% TMD, CLASS E RDX; ρ_o = 1.25 g/cc, DISTANCE-TIME DATA (KEY OF FIGURE 4a).

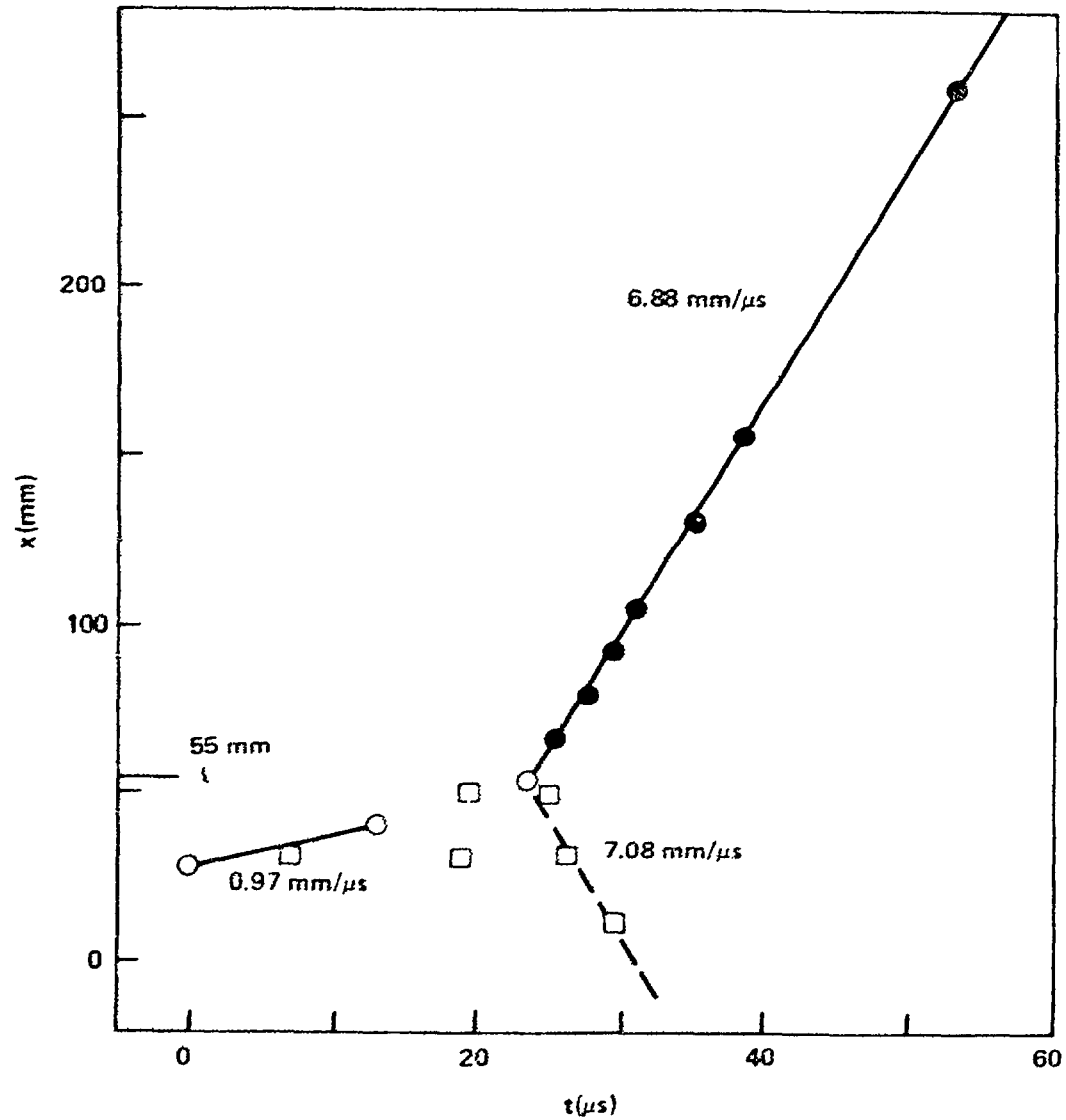

a. DISTANCE-TIME DATA (KEY OF FIGURE 4a).

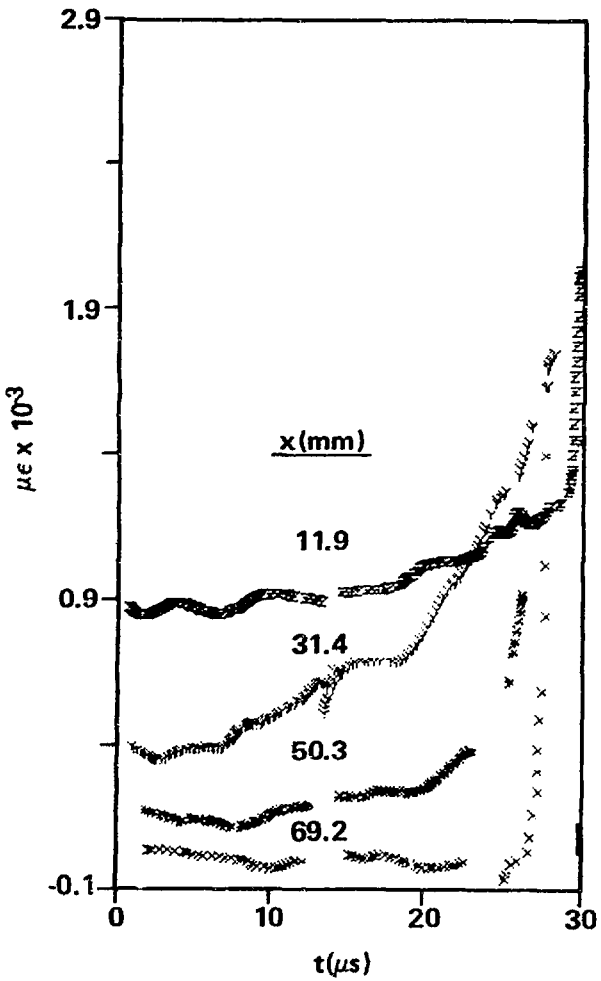

b. STRAIN-TIME DATA (KEY OF FIGURE 4b).

FIG. C3. SHOT 910 ON 69.1% TMD, CLASS E RDX; ρ_o = 1.25 g/cc.

APPENDIX D

Detailed Data for Waxed RDX and Waxed HMX

The first RDX/wax series was reported in reference 1. Since the SG records were either missing or very poor, they were not reproduced there. All those of the present series are reproduced here, and most are good records. Data for the waxed RDX appear in Table D1; those for the two waxed HMX series, in Tables D2 and D3. They are plotted in Figures D1-D14. As was remarked above, most of the strain gage records obtained were good. In particular, they illustrate the effect of rapid pressure buildup.

A sharp dip in the ε-t record, i.e. negative dP/dt, and a minimum is associated with appearance of a shock. If the SG is located at $x \lesssim \ell$, it is apt to be destroyed e.g. Fig. D4b, SG at 168 mm and Fig. D9b, SG at 143 mm. If the SG is at $x > \ell$, the same type of dip appears before the gage is destroyed, e.g., Fig. D1b, SG at 79.3 mm. If $x < \ell$, SG records frequently show a dip which strengthens as x approaches ℓ, e.g., D5b and D9b. In this last case, the minima are associated with shock formation and time readings are taken at the beginning of the dip and at the minimum; both readings are plotted on the space-time illustration because we believe they bracket the actual time of the pressure excursion.

Within this group of records, there is no instance in which the IP discharge seems to be affected by shock formation. However, this does occur occasionally. We do have one record (Fig. D10a) showing peculiar pin discharge times. The companion SG records (Fig. D10b) show appreciable electromagnetic noise and interference in the interval 280-460μs which includes the questionable discharges. Hence we attribute them to EM disturbance.

As might be expected, both waxed series conform to the physical model of DDT developed for 91/9 RDX/wax.

Table D1. Detailed Data for RDX/Wax Series

Shot Number:	404		411		405		415		505	
Density:										
g/cc	1.248		1.222		1.170		1.402		1.364	
% TMD	70.9		72.6		71.3		85.2		84.9	
% Wax	3.0		9.0		12		12		15	
IP Data:	x	t	x	t	x	t	x	t	x	t
	28.95	0.0*	41.1	0.0*	41.4	0.0*	28.19	0.0*	41.40	0.0*
	54.1	53.7*	66.5	155.0*	54.1	57.05*	41.40	34.19*	79.50	78.06*
	66.8	64.2	104.8	291.0	79.6	-	54.10	59.94*	117.60	160.05*
	79.5	65.7	130.2	362.4	105.0	-	79.37	112.92*	143.00	212.91*
	92.2	67.8	155.7	435.8	130.4	-	104.90	154.59*	168.40	257.29
	105.0	69.6	181.1	501.8	155.8	400.8	130.30	196.39	193.80	304.41
	130.55	73.3	206.5	540.2 or 551.0	181.2	475.9	155.70	224.19	206.50	325.51
	155.95	77.3	231.9	555.6	206.6	-	181.10	231.30	225.55	347.79
	206.75	84.75	244.1	557.4	232.0	617.45	206.50	235.47	244.60	345.35
	257.55	92.0	263.4	558.9	257.4	685.6	257.30	242.32	263.65	349.42
SG Data:	x	t_{PC}	x	t_{PC}	x	t_{PC}	x	t_{PC}	x	t_{PC}
	28.5	24	92.2	463	28.6	No PC	20.3	121	20.32	200
	54.3	50	142.8	521-533	105.0	Wave	79.5	169	79.37	250
	79.3	67.3			206.3	found	130.3	197	117.60	280
							168.4	216	155.45	290-308
									193.93	315-326
ℓ(mm):	72^{-5}_{+0}		220^{+0**}_{-14}		F		176±5		232±3	
D(mm/μs):	6.77		>7.2		F		>7.47		>4.68	
σ(mm/μs):	0.04		-				-		-	

*Custom-made probe
**176 mm from tube fragments
>206 mm from IP record
Units of x and t are mm and μs, respectively.

Table D2. Detailed Data for HMX/wax Series Prepared from Narrow Sieve Cut ($\delta \sim 115\mu$) HMX

Shot Number:	1605		1610		1608		1611		1615	
Density g/cc:	1.322		1.307		1.267		1.229		1.188	
% TMD:	69.4		70.3		70.4		69.9		69.4	
% Wax	0.0		3.0		6.0		9.0		12.0	
IP Data:	x	t	x	t	x	t	x	t	x	t
	16.1	0.0*	29.0	0.0*	28.8	0.0*	41.5	0.0*	66.2	0.0
	28.8	14.3*	41.7	24.7*	41.5	33.75*	60.6	52.9*	91.6	70.1
	41.5	18.25*	54.4	42.9*	54.4	61.7*	79.6	97.9*	117.0	136.85
	54.2	20.2	79.9	53.1*	79.8	110.5*	105.0	156.5*	142.4	188.4
	66.9	21.95	105.3	56.45*	105.2	122.6	130.4	191.2*	167.8	262.4
	79.6	24.2	130.7	59.6	130.6	125.7	155.8	198.0	186.9	349.3
	92.2	25.85	156.1	63.0	156.0	129.3	181.2	202.6	206.0	439.0
	105.0	27.65	181.5	66.8	181.4	132.75	206.6	206.7	225.0	452.0
	130.4	31.25	207.0	70.7	206.8	137.15	232.0	210.8	244.1	481.9
	257.4	50.1	257.8	77.7	257.6	144.7	263.9	215.5	263.1	519.7
SG Data:	x	tpc	x	tpc	x	tpc	x	tpc	x	tpc
	12.2	4.6	12.2	–	20.6	44.5	20.6	–	20.4	–
	31.2	7.8	31.2	19.8	54.4	76.5	54.1	98	92.2	–
	50.3	20.7**	50.4	29.1	79.8	101.0	92.2	170.4	117.7	383
	69.3	21.7**	69.7	48.1,54	105.0	120.7	117.7	182.0	149.4	436
			88.6	51.2-57.0	124.2	128.0	143.0	192.0	181.4	480
ℓ(mm):	35±1		67±1		99±1		143±1		273±2	
D(mm/μs):	6.80		~7.2		6.63		~6.4		–	
σ(mm/μs)	0.04		–		0.13		–		–	

*Custom-made probe

**Minima and correspond (±1 μs) to passage of detonation wave

Table D3. Detailed Data for HMX/Wax Series Prepared from Class A HMX

Shot Number:	1616	1617	1618	1701
Density g/cc:	1.322	1.273	1.225	1.195
%TMD:	69.4	70.4	69.9	69.3
% Wax	0.0	6.0	9.0	12.0
IP Data:	x̄ / t̄	x̄ / t̄	x̄ / t̄	x̄ / g̃
	16.0 / 0.0*	29.0 / 0.0*	41.7 / 0.0*	67.1 / 0.0*
	28.7 / 29.75*	41.7 / 54.2*	60.8 / 84.8*	92.5 / 93.7*
	41.4 / 39.6*	55.4 / 93.6	79.9 / 142.3*	118.0 / 168.7*
	54.1 / 42.25*	67.1 / 127.8*	105.3 / 210.1*	143.4 / 244.5*
	66.9 / 43.8	86.1 / 166.05*	130.7 / 267.1	168.8 / 316.05
	79.6 / 45.35	105.2 / 192.0	156.2 / 322.7	194.2 / 382.3
	92.3 / 47.1	124.2 / 199.2	181.6 / 371.1	219.6 / 449.45
	105.0 / 49.15	143.3 / 202.0	207.0 / 388.8	245.1 / 516.95
	130.4 / 52.45	168.7 / 205.9	232.4 / 392.7	264.0 / 567.1
	257.4 / 71.0	264.0 / 218.6	264.3 / 397.25	
SG Data:	x̄ / tPC	x̄ / tPC	x̄ / tPC	x̄ / tPC
	12.3 / 21.1	20.6 / 96	20.4 / –	20.4 / –
	31.4 / 32.4-37.6	48.0 / 126	54.2 / 246	79.5 / 591
	50.4 / 40.5-44.5	67.1 / 151	85.9 / 290	117.6 / 600
	69.5 / 41.6-45.3	105.2 / –	117.9 / 310	149.4 / 637
			143.0 / 343-357	181.4 / 675
ℓ(mm):	45±1	119±1	210±1	F
D(mm/μs):	∿6.9	∿7.1	∿6.7	F
σ(mm/μs):	–	–	–	

*Custom-made probe

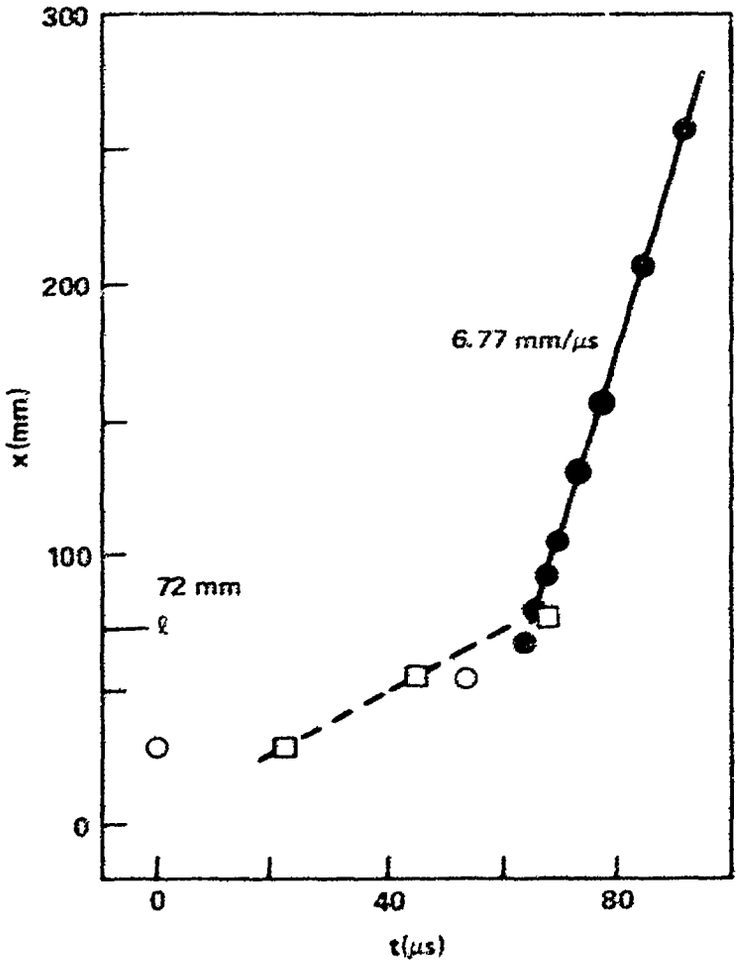

a. DISTANCE-TIME DATA (KEY OF FIGURE 4a).

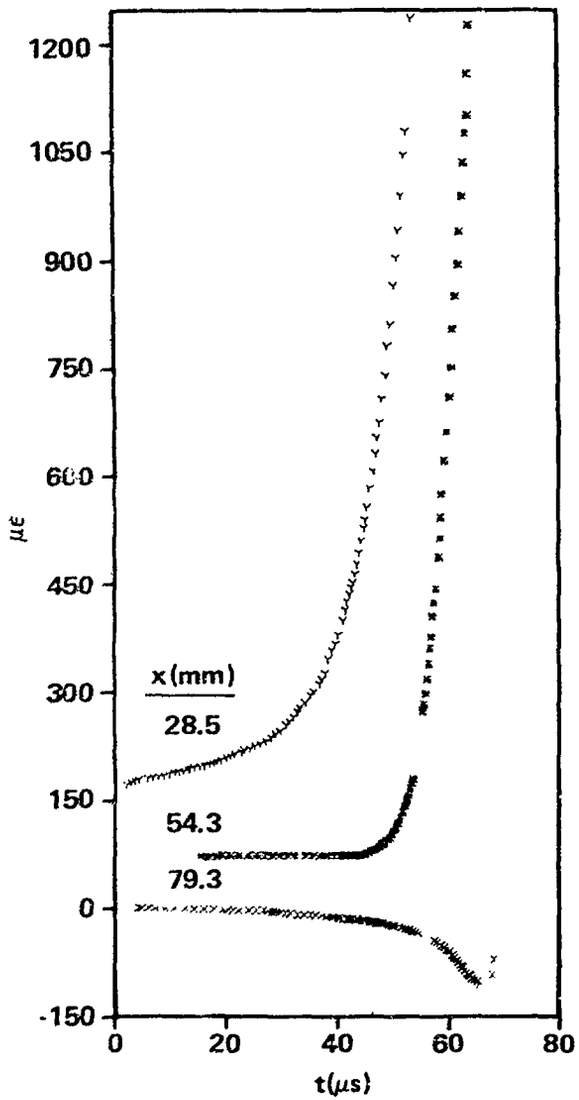

b. STRAIN-TIME DATA (KEY OF FIGURE A1b).

FIG. D1. SHOT 404 ON 70.9% TMD 97/3 RDX/WAX, ρ_o = 1.25 g/cc.

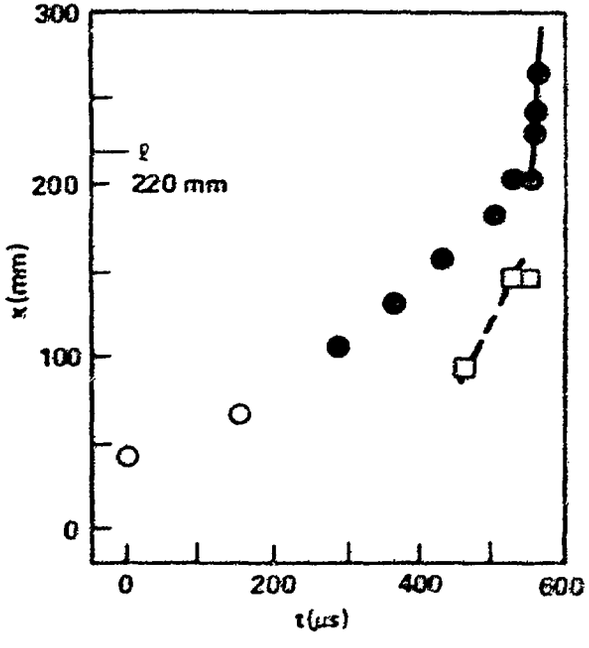

a. DISTANCE-TIME DATA (KEY OF FIGURE 4a).

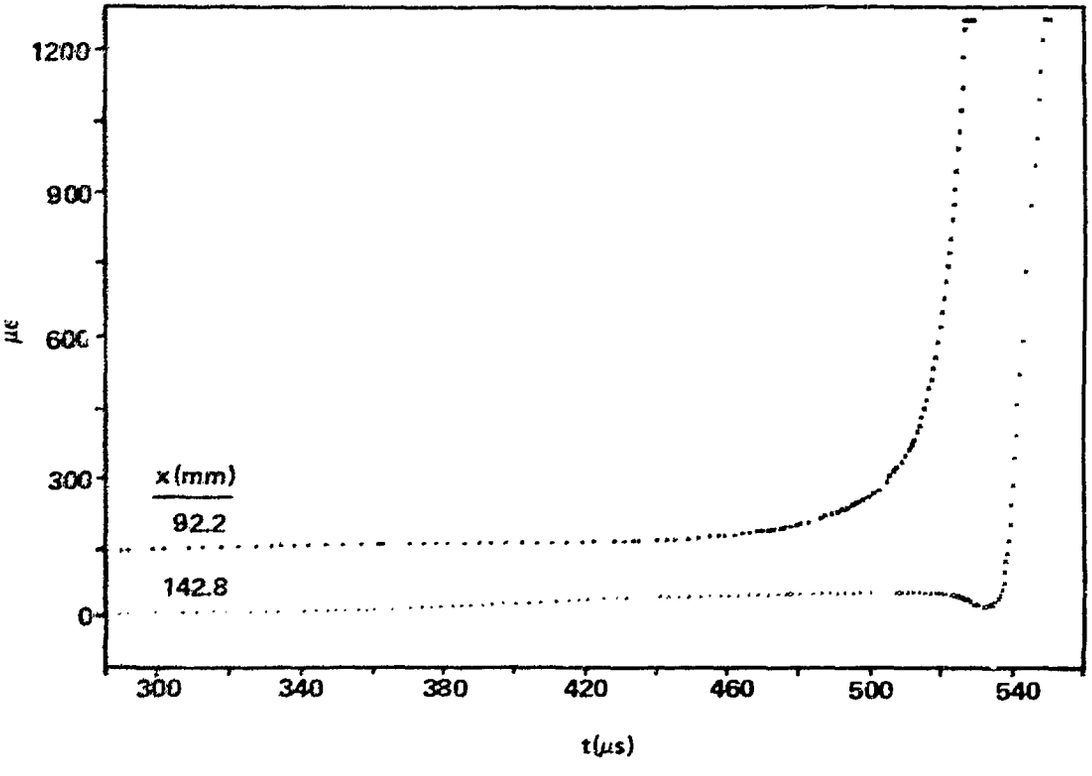

b. STRAIN-TIME DATA (KEY OF FIGURE A1b).

FIG. D2. SHOT 411 ON 70.3% TMD 91/9 RDX/WAX, ρ_o = 1.22 g/cc.

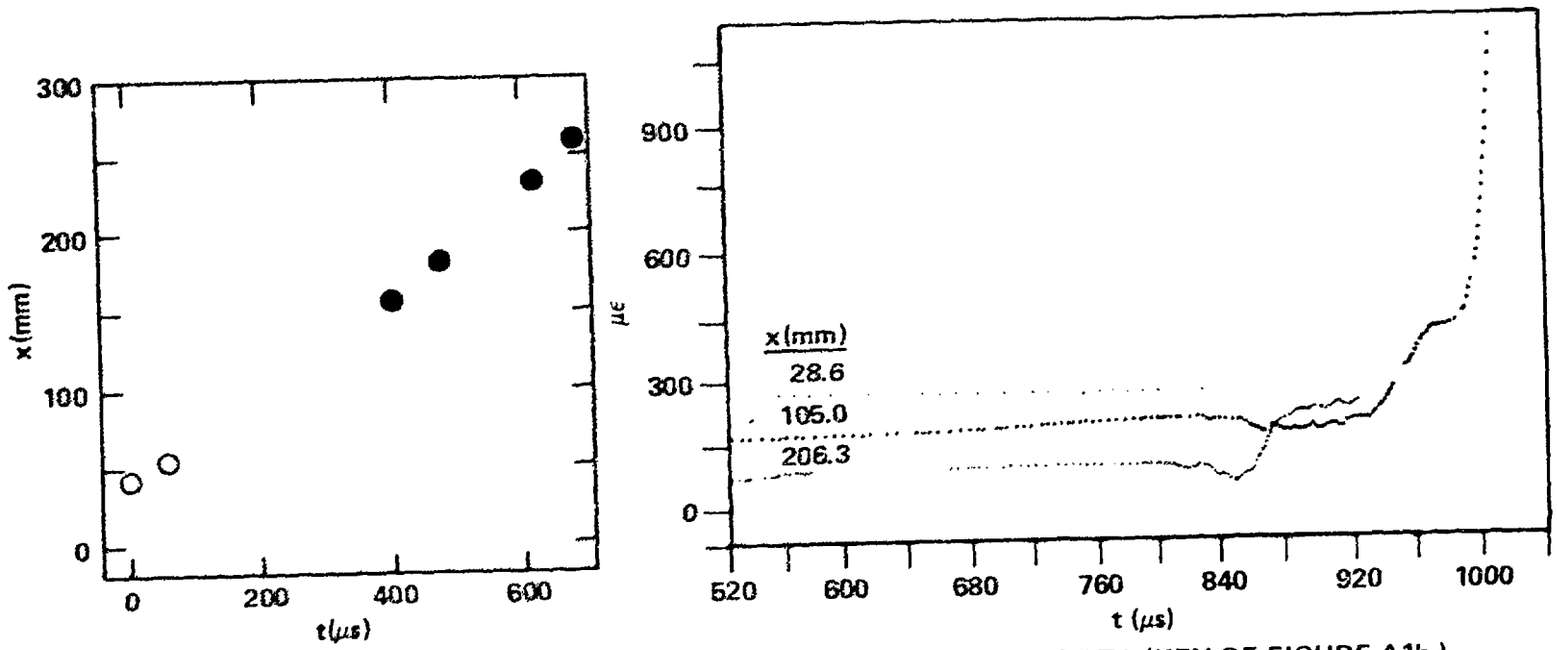

a. DISTANCE-TIME DATA (KEY OF FIGURE 4a)

b. STRAIN-TIME DATA (KEY OF FIGURE A1b.)

FIG. D3. SHOT 405 ON 71.3% TMD 88/12 RDX/WAX, ρ_o = 1.25 g/cc.

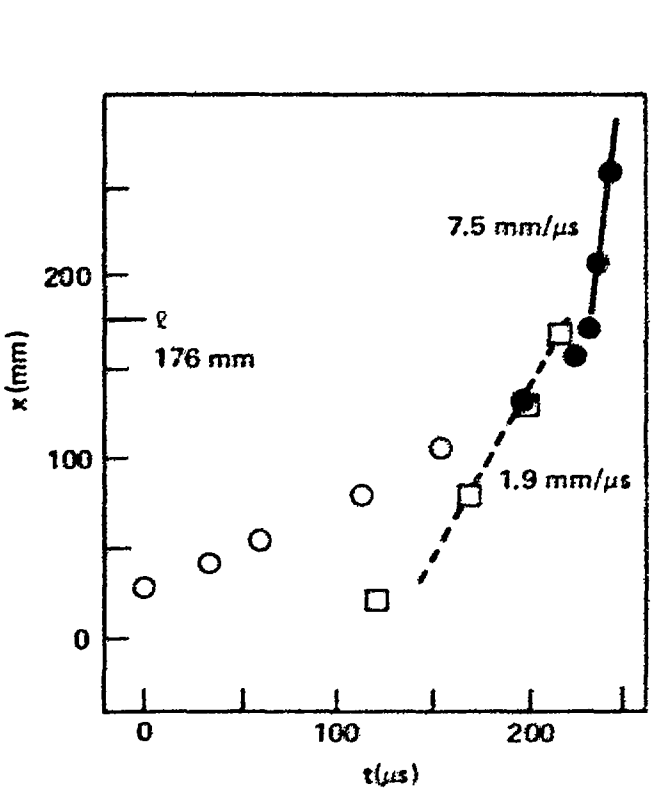

a. SPACE-TIME DATA (KEY OF FIGURE 4a).

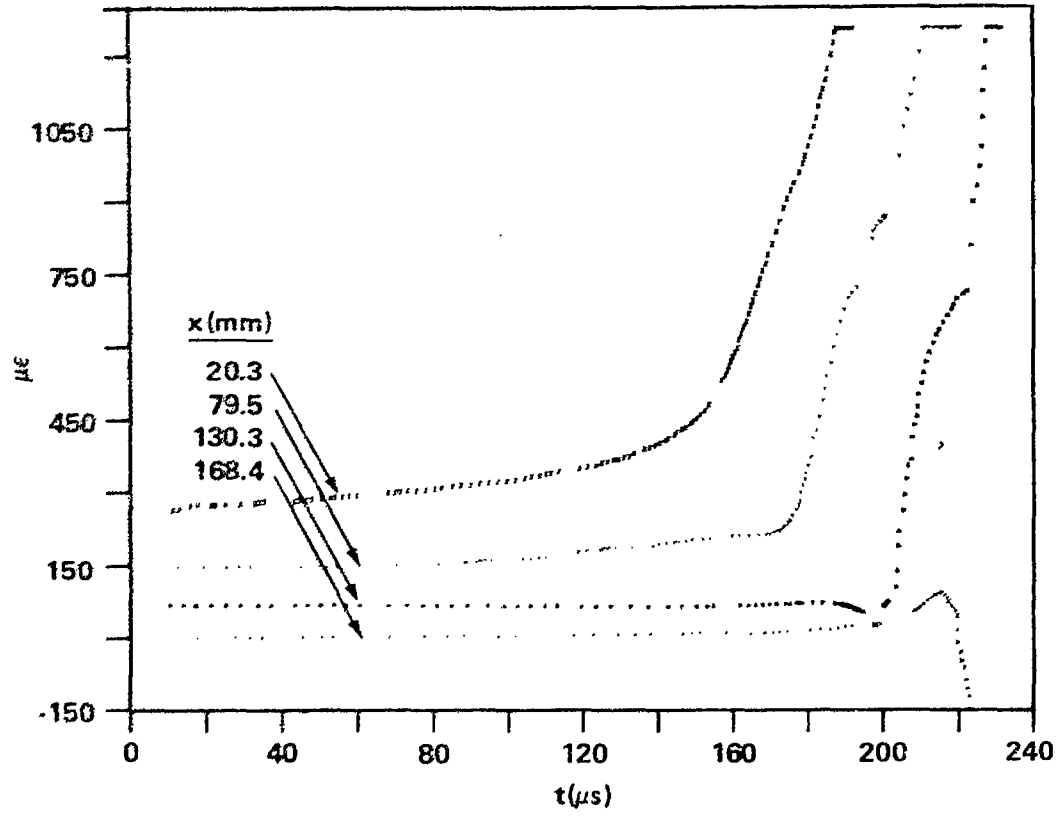

b. STRAIN-TIME DATA (KEY OF FIGURE A1b).

FIG. D4. SHOT 415 ON 85.2% TMD 88/12 RDX/WAX, ρ_o = 1.40 g/cc.

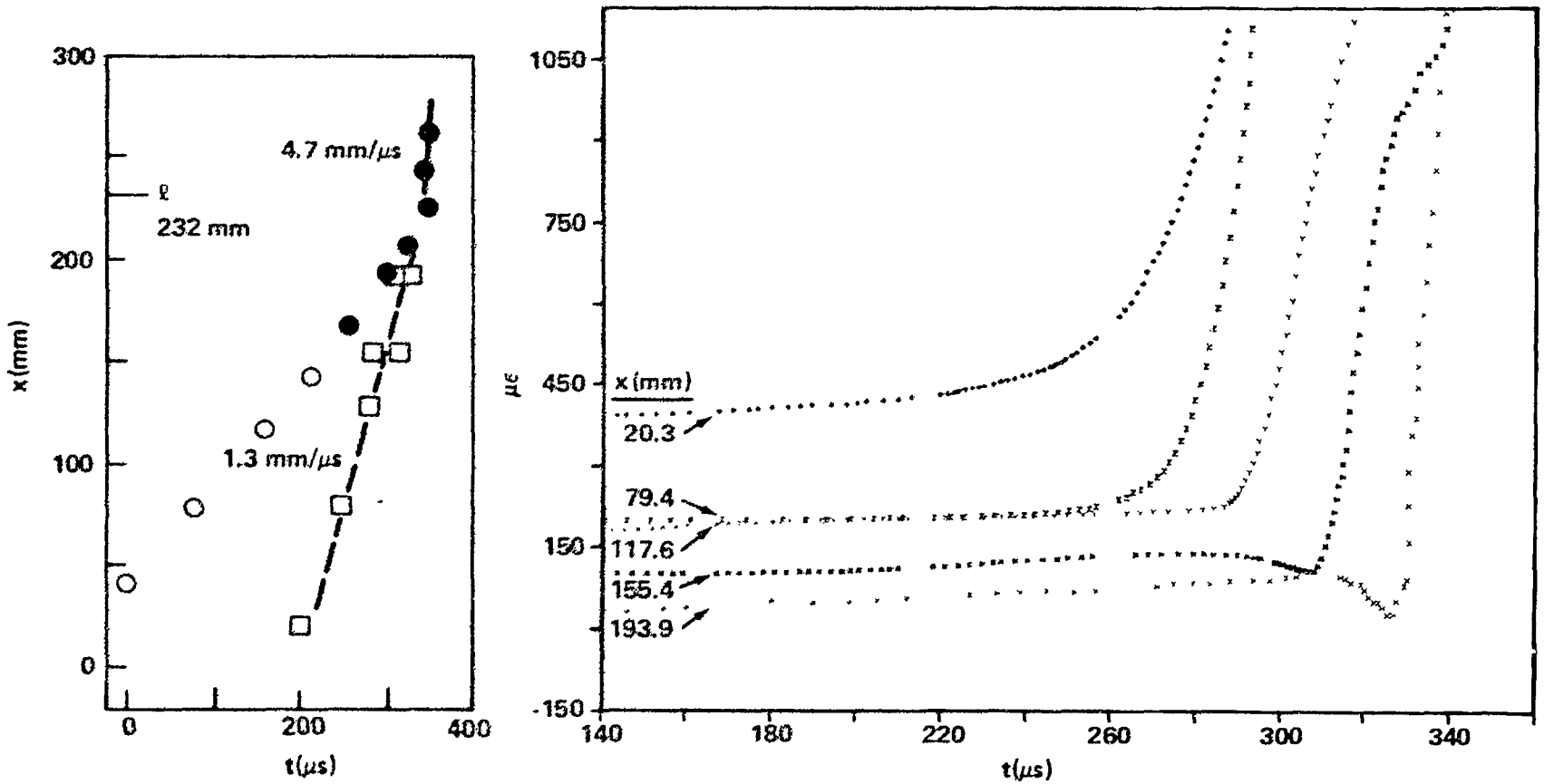

a. SPACE-TIME DATA (KEY OF FIGURE 4a).

b. STRAIN-TIME DATA (KEY OF FIGURE A1b).

FIG. D5. SHOT 505 ON 85% TMD 85/15 RDX/WAX, ρ_o = 1.36 g/cc.

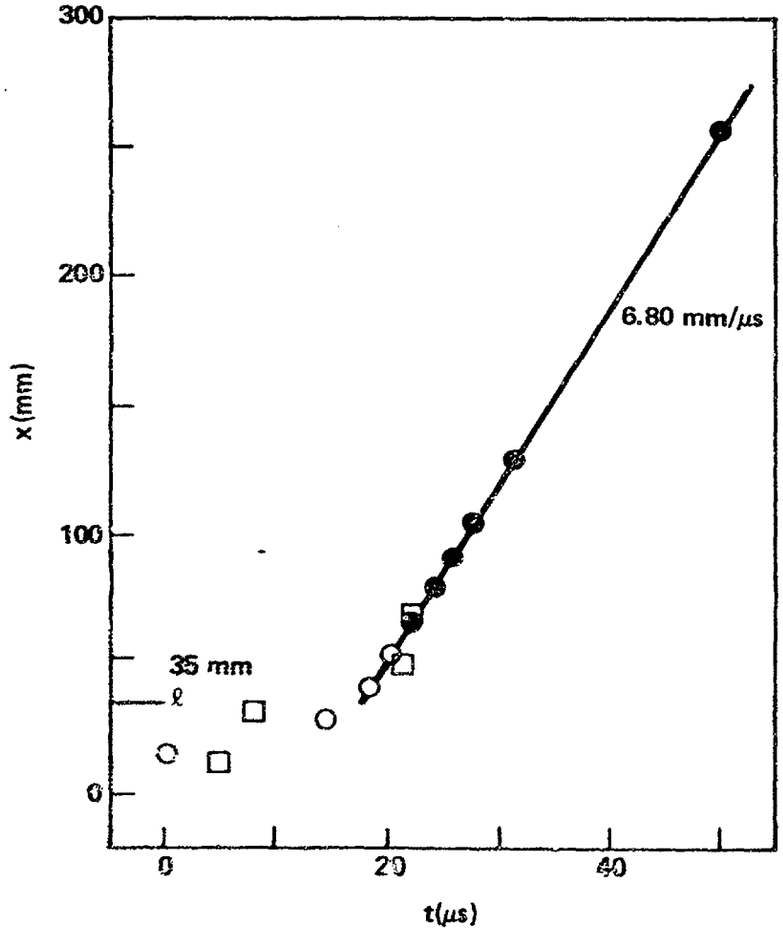

a. DISTANCE-TIME DATA (KEY OF FIGURE 4a).

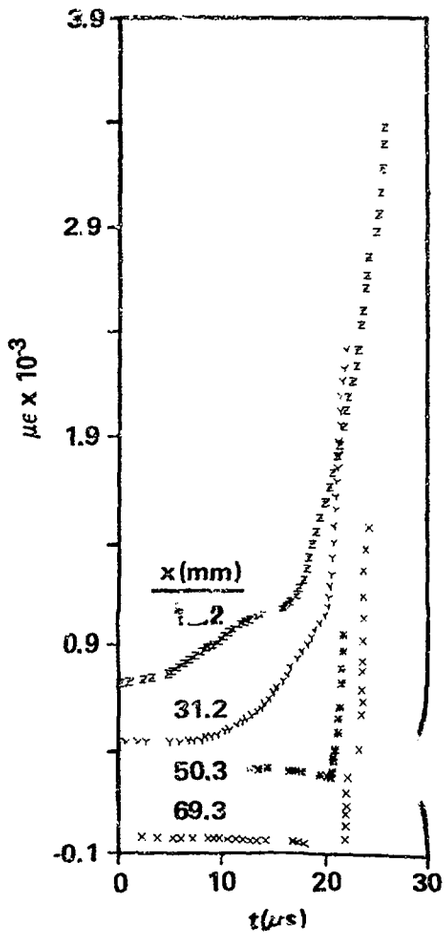

b. STRAIN-TIME DATA (KEY OF FIGURE 4b).

FIG. D6. SHOT 1605 ON PBX HMX AT 69.4% TMD, ρ_o = 1.32 g/cc.

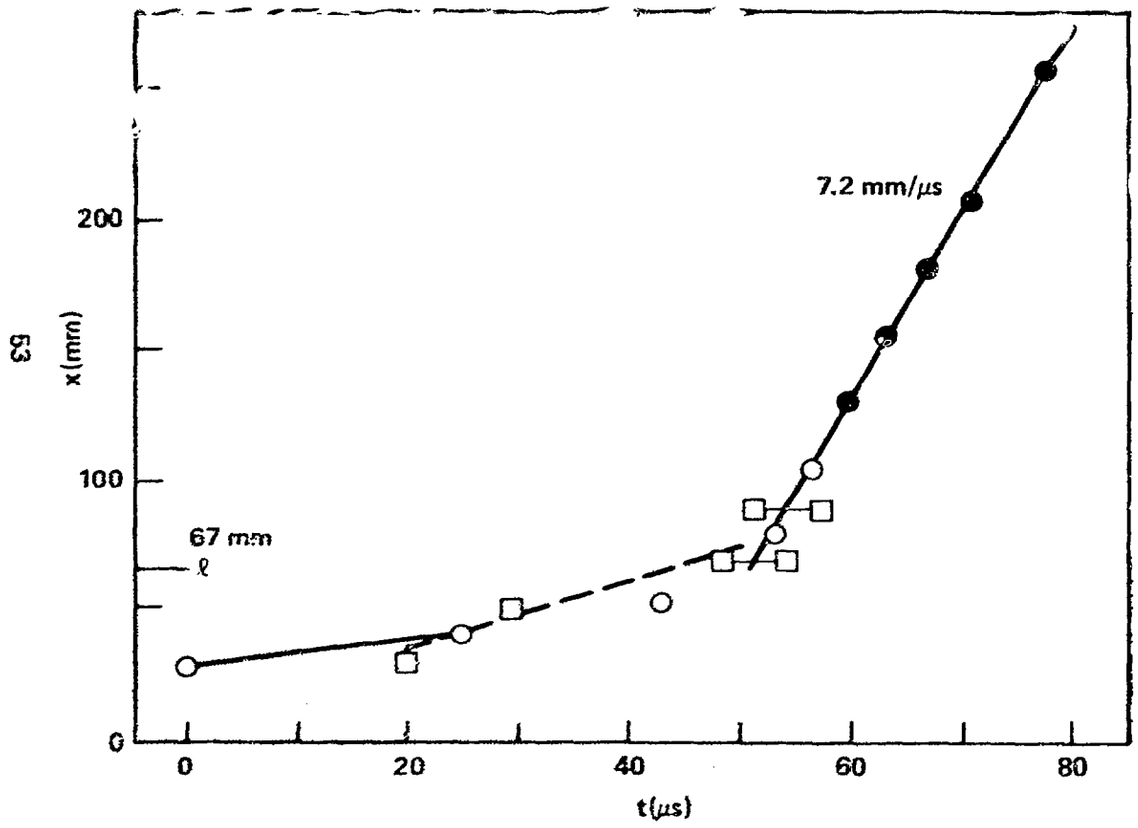

a. DISTANCE-TIME DATA (KEY OF FIGURE 4a).

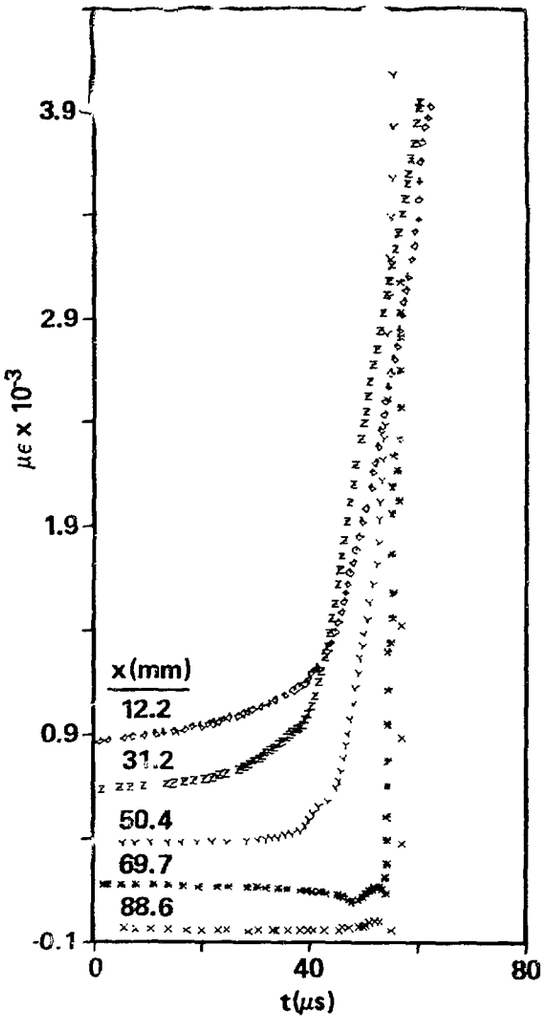

b. STRAIN-TIME DATA (KEY OF FIGURE 4b).

FIG. D7. SHOT 1610 ON 70.7% TMD 97/3 115μ-HMX/WAX, ρ_o = 1.31 g/cc.

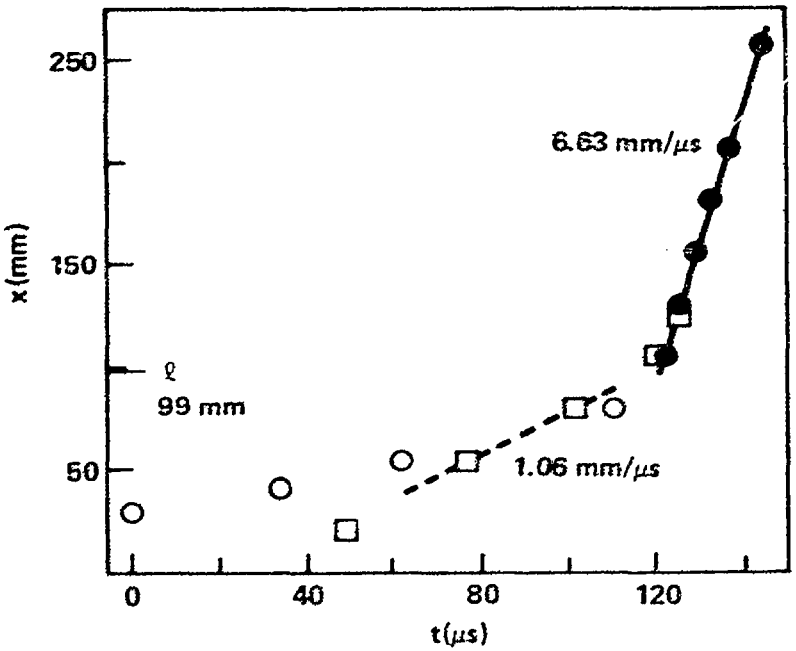

a. DISTANCE-TIME DATA (KEY OF FIGURE 4a).

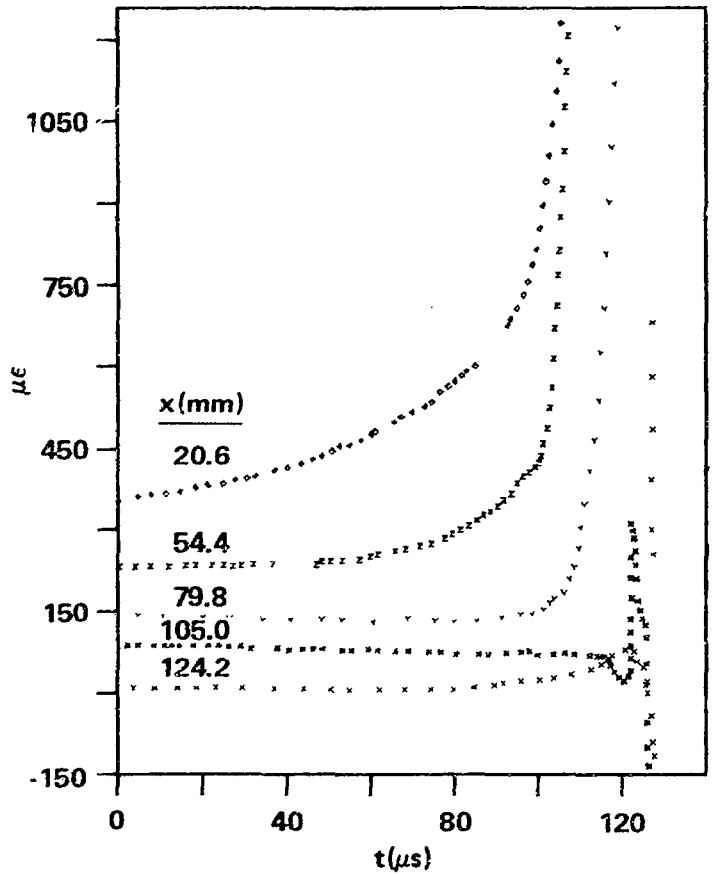

b. STRAIN-TIME DATA (KEY OF FIGURE A1b).

FIG. D8. SHOT 1608 ON 70.4% TMD 94/6 115μ-HMX/WAX, ρ_o = 1.27 g/cc.

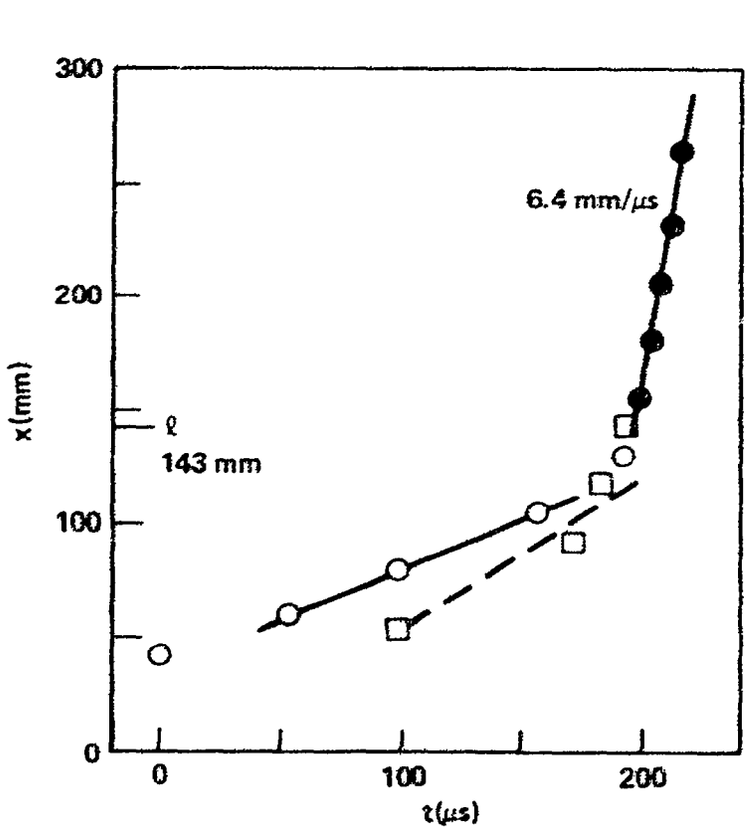

a. DISTANCE-TIME DATA (KEY OF FIGURE 4a).

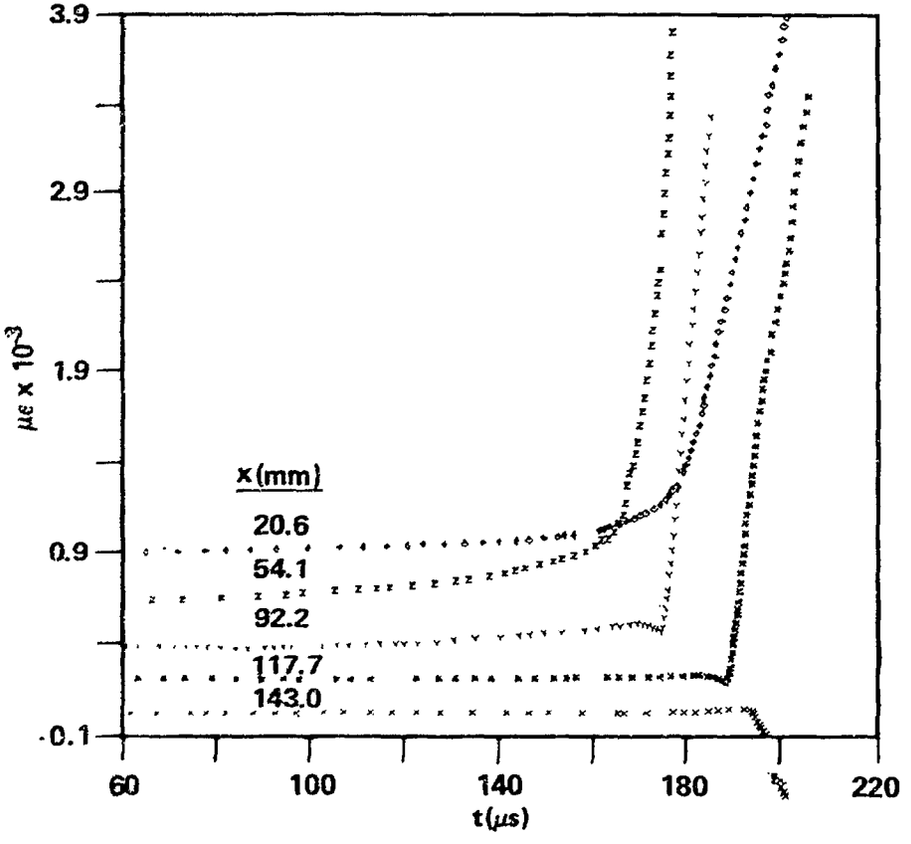

b. STRAIN-TIME DATA (KEY OF FIGURE 4b).

FIG. D9. SHOT 1611 ON 69.9% TMD 91/9 115μ-HMX/WAX, ρ_o = 1.23 g/cc.

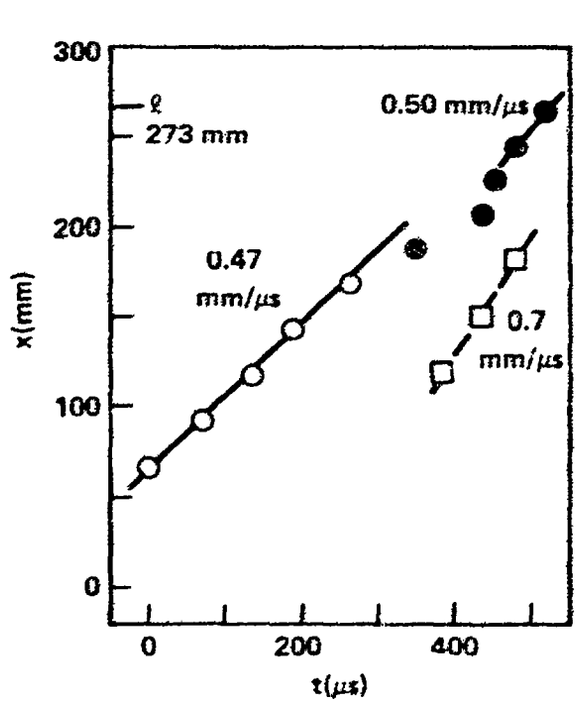

a. DISTANCE-TIME DATA (KEY OF FIGURE 4a).

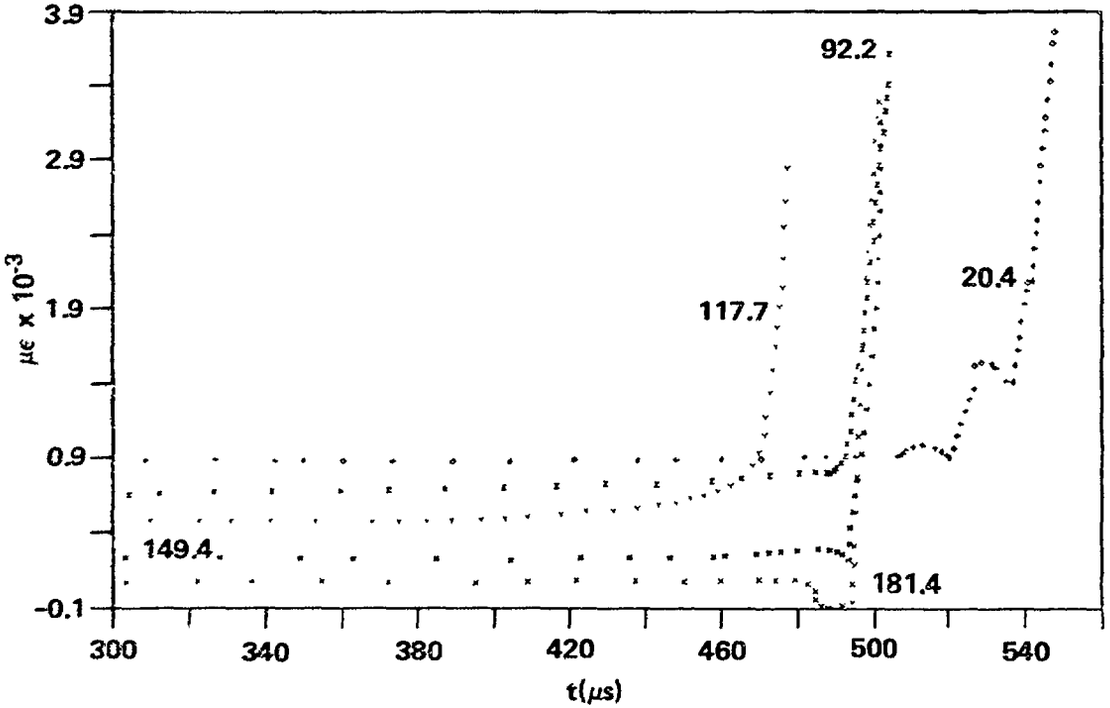

b. STRAIN-TIME DATA (KEY OF FIGURE 4b).

FIG. D10. SHOT 1615 ON 69.3% TMD 88/12 115μ-HMX/WAX, ρ_o = 1.19.

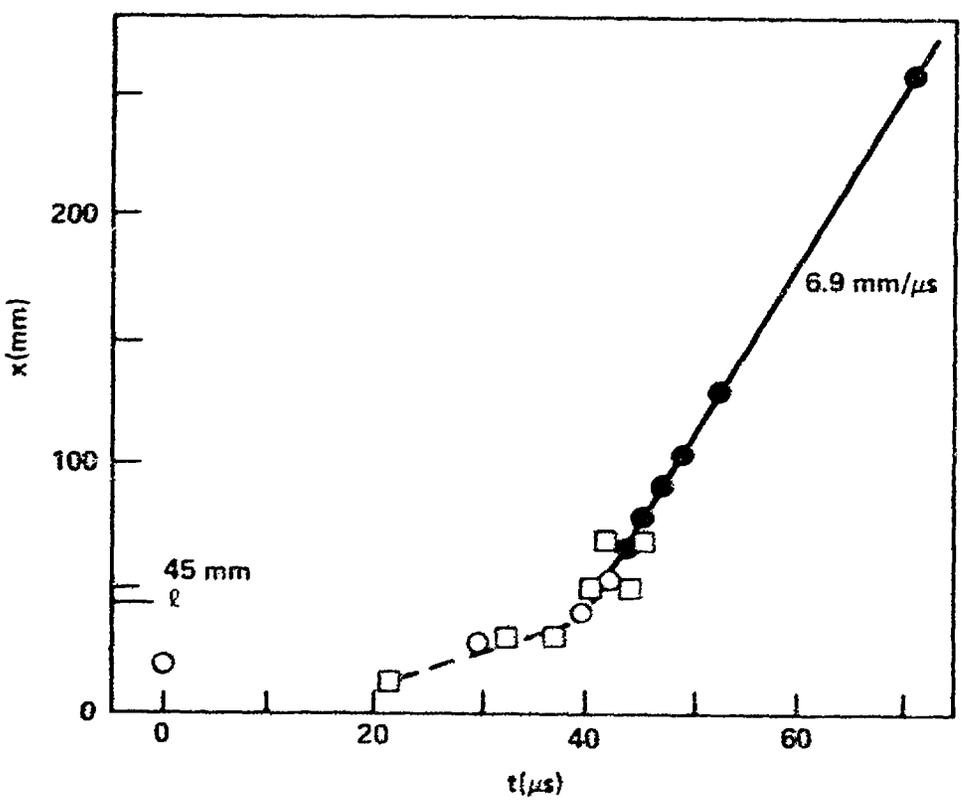

a. DISTANCE-TIME DATA (KEY OF FIGURE 4a).

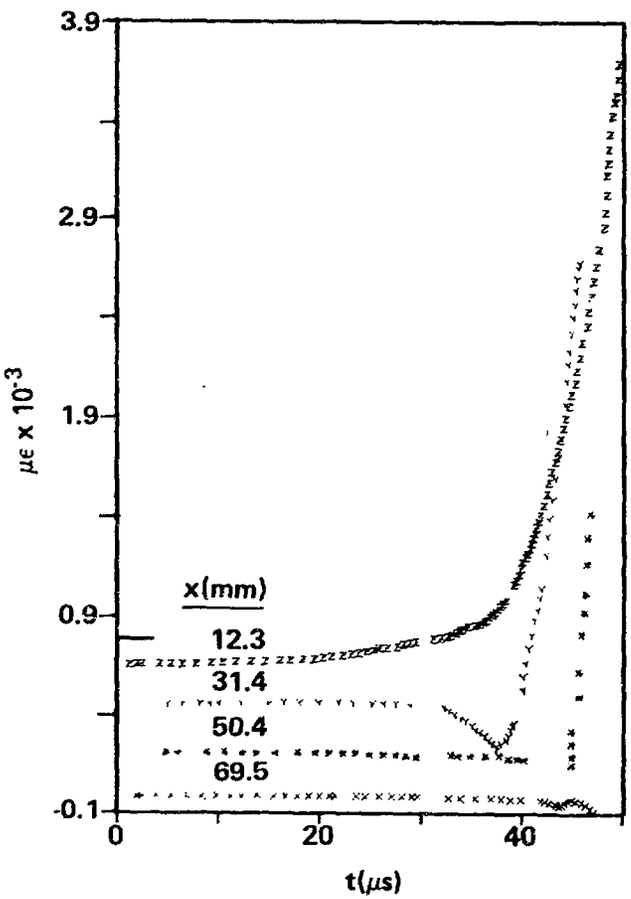

b. STRAIN-TIME DATA (KEY OF FIGURE 4b).

FIG. D11. SHOT 1616 ON 69.4% HMX (A), ρ_o = 1.32 g/cc.

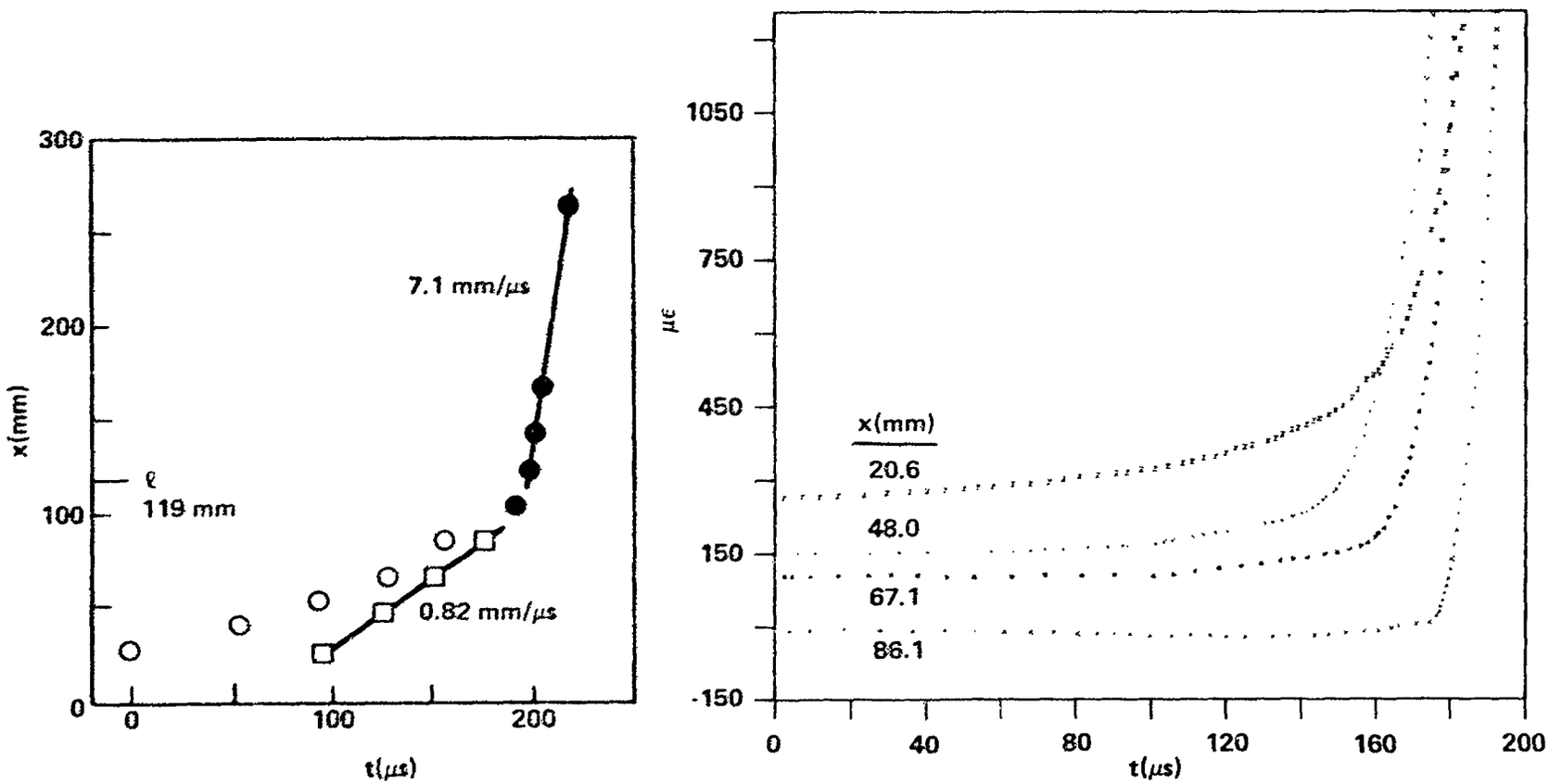

a. DISTANCE-TIME DATA (KEY OF FIGURE 4a).

b. STRAIN-TIME DATA (KEY OF FIGURE A1b).

FIG. D12. SHOT 1617 ON 70.4% TMD 94/6 HMX (A)/WAX, ρ_o = 1.27 g/cc.

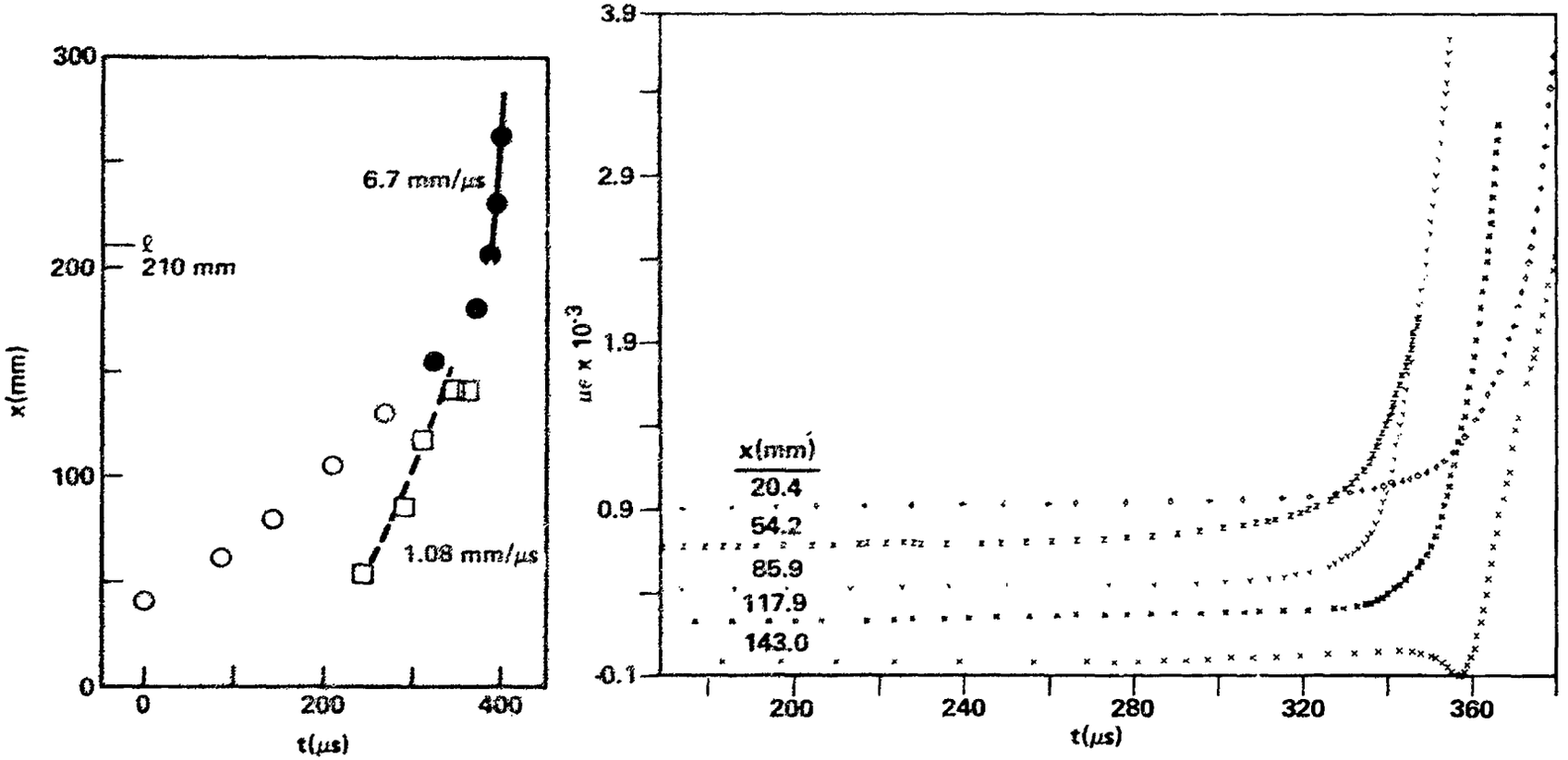

a. DISTANCE-TIME DATA (KEY OF FIGURE 4a).

b. STRAIN-TIME DATA (KEY OF FIGURE 4b).

FIG. D13. SHOT 1618 ON 69.4% TMD 91/9 HMX (A)/WAX, ρ_o = 1.22 g/cc.

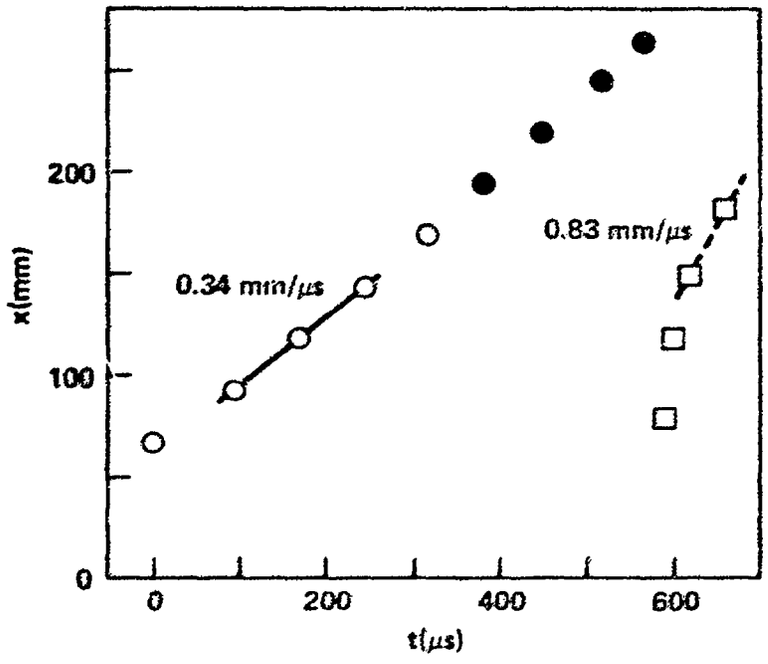

a. DISTANCE-TIME DATA (KEY OF FIGURE 4a).

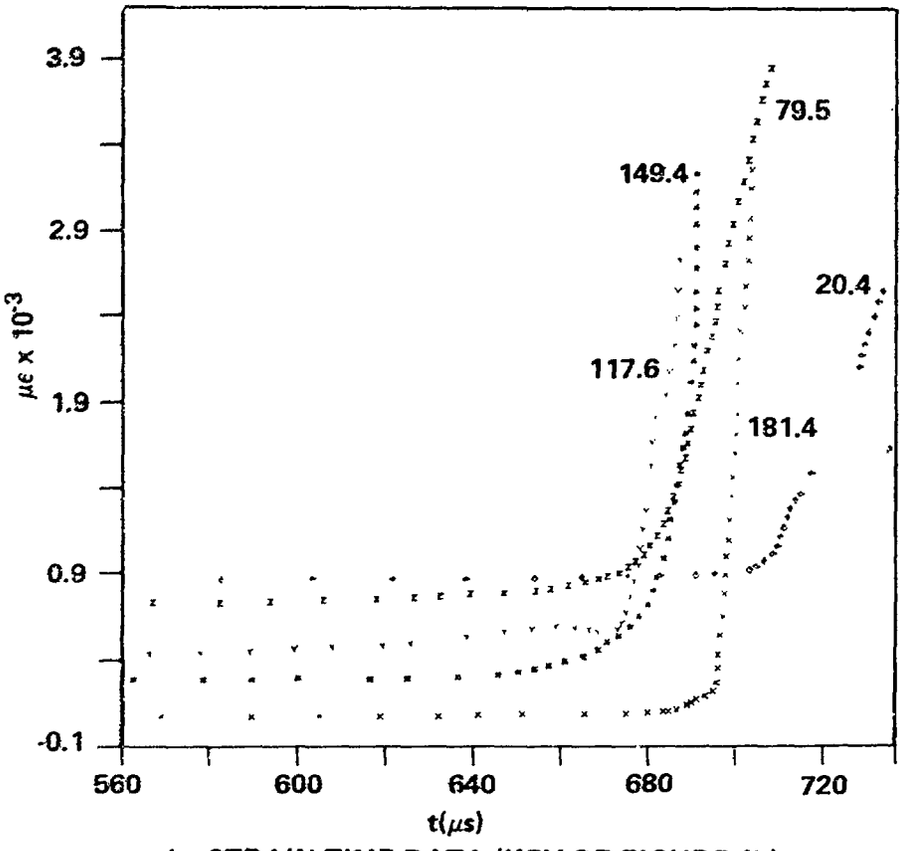

b. STRAIN-TIME DATA (KEY OF FIGURE 4b).

FIG. D14. SHOT 1701 ON 69.4% TMD 88/12 HMX (A)/WAX, ρ_o = 1.19 g/cc.

APPENDIX E

DDT Data for Waxed Tetryl

Two shots on waxed tetryl are reported here; the detailed data appear in Table E-1. Shot 618 was made at 75% TMD of 91/9 tetryl/wax. This material ignited and showed convective flame spread initially at 0.3 mm/μs, with decreasing speed until its failure somewhere beyond x = 80 mm and before x = 105 mm, the location of the first IP which showed no response. It did not, of course, exhibit DDT (see Fig. E1). This waxed tetryl is considerably less susceptible to transition in our setup than is the comparably waxed RDX at 75% TMD(1).

Shot 1606, 69.4% TMD 97/3 tetryl/wax was made to assess further the results already reported on this mixture(4). The present results, plotted in Figure E2 confirm the previous ones in value of ℓ(227 vs 238 & 258 mm), rate of convective flame spread (0.3 vs. 0.2 mm/μs), and apparent conformity to the transition mechanism devised for 91/9 RDX/wax. It differs only in the velocity of the PC front (2.4 vs 1.6 mm/μs) which is attributed to a greater compaction of this charge during the initial slow burning. (The difference could result from a difference in the properties of the confining tubes used in the two cases. Although tubes are bought under specifications, they are not tested for strength prior to use.) However, the qualitative pattern of SG curves in both shots of reference 4 and of those in Figure E2b is very similar. The evidence to date indicates that addition of 3% wax to the coarse tetryl has modified the initial portion of the transition so that it now comforms to the physical model of DDT(1).

Table E1. Detailed Data for Waxed Tetryl Shots

Shot No:	1606		618	
Density				
g/cc:	1.174		1.210	
% TMD:	69.4		74.6	
ρ_v g/cc	1.692		1.623	
% Wax	3.0		9.0	
IP Data:	x	t	x	t
	54.1	0.0*	28.7	0.0*
	79.5	29.8*	41.4	50.85*
	104.9	105.9*	54.1	113.6*
	130.3	196.35*	66.8	166.8*
	155.8	256.3*	79.6	340.9
	181.8	304.2*	105.0	-
	206.5	337.35*	130.4	-
	225.7	347.55*	156.0	-
	244.7	351.15	181.4	-
	263.8	354.2	257.6	-
SG Data:	79.6	293.5	Very little output; records not read.	
	117.5	296.5		
	149.6	310		
	181.2	336.5		
	206.5	334		
ℓ(mm)	227±1		F**	
D(mm/μs)	6.3		F	
Predet. Front Velocities (mm/μs):	0.3, 2.4		0.3 to 0	
Δt_D(μs)	>248		F	

* Custom-made probes
**Failure

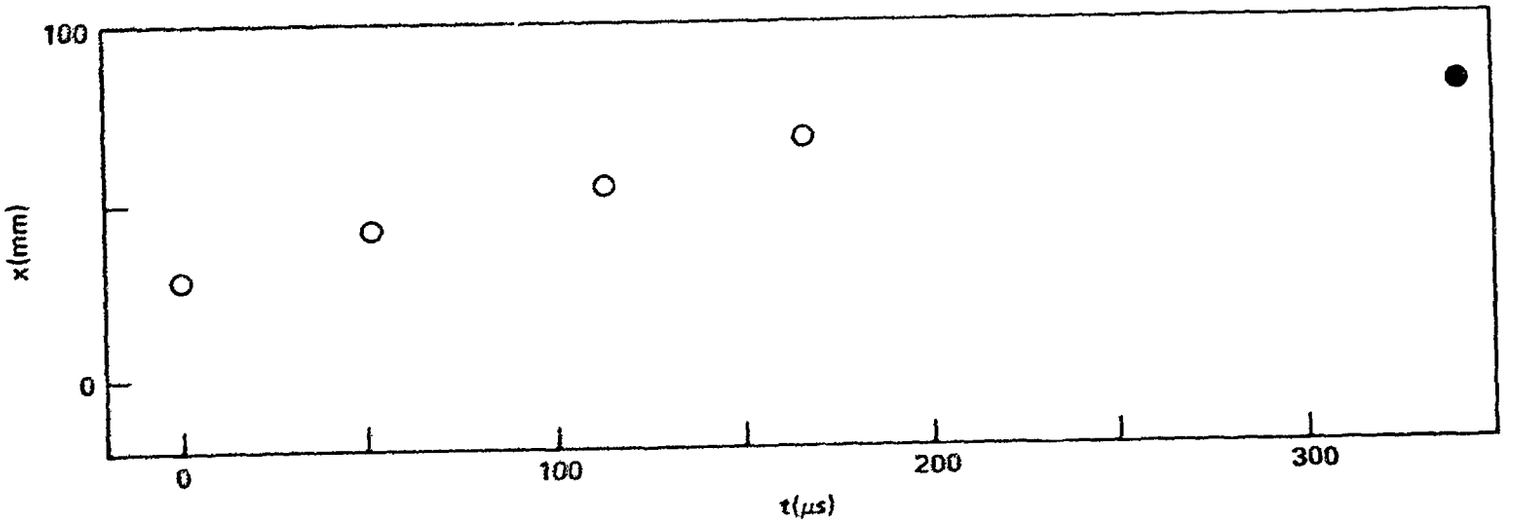

FIG. E1. SHOT 618 ON 74.6% TMD 91/9 TETRYL/WAX, ρ_o = 1.21 g/cc: DISTANCE-TIME DATA (KEY OF FIGURE 4a).

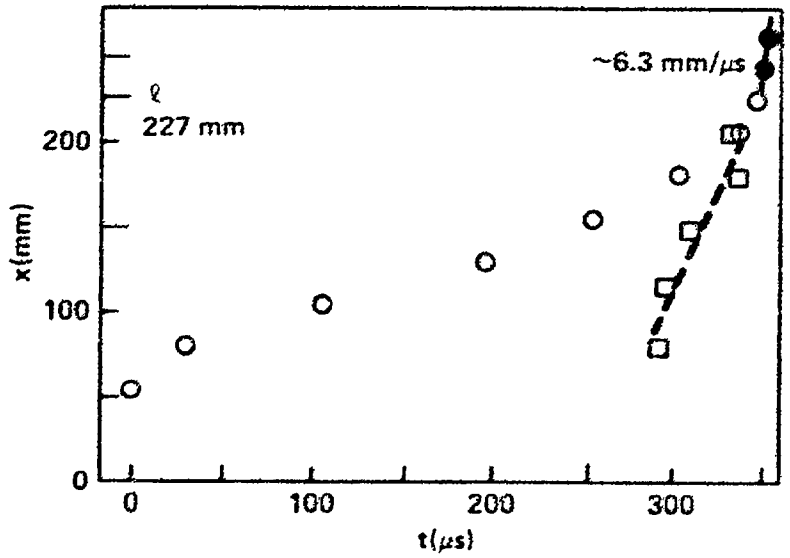

a. DISTANCE-TIME DATA (KEY OF FIGURE 4a)

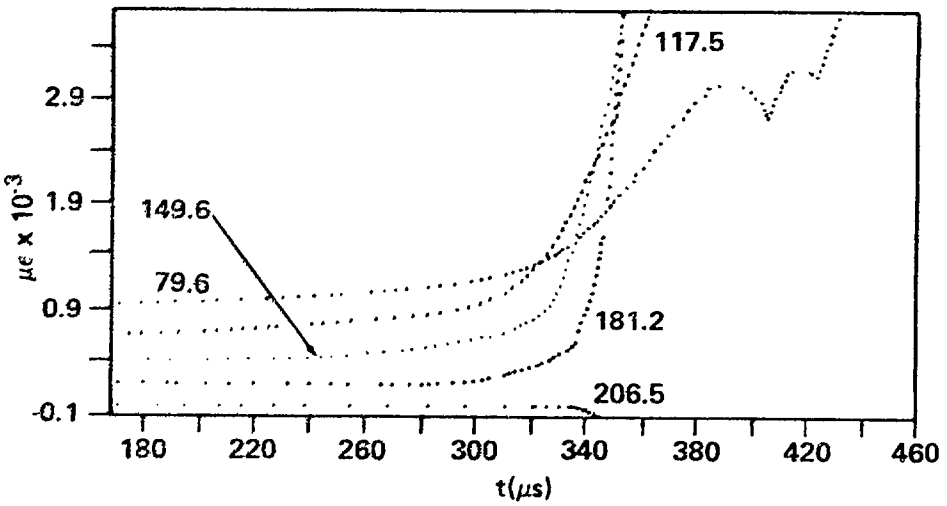

b. STRAIN-TIME DATA (KEY OF FIGURE 4b)

FIG. E2. SHOT 1606 ON 69.4% TMD 97/3 TETRYL/WAX, ρ_o = 1.69 g/cc.

DISTRIBUTION LIST

	Copies
Chief of Naval Material Washington, DC 20360	
Commander Attn: AIR-350 AIR-330 Naval Air Systems Command Department of the Navy Washington, DC 20361	
Commander Attn: SEA-09G32 SEA-0332 SEA-0331 SEA-03B SEA-031 Naval Sea Systems Command Department of the Navy Washington, DC 20360	2 3
Director Attn: SP-273, R. M. Kinert SP-27311, E. L. Throckmorton, Jr. Strategic Systems Project Office (PM-1) Department of the Navy Washington, DC 20376	
Office of Naval Research Attn: Rear Admiral C. O. Holmquist Technical Library (ONR-741) Department of the Navy Arlington, VA 22217	

DISTRIBUTION (Cont.)

Copies

Commander
Attn: Code 556
Technical Library
H. D. Mallory
Code 452
Code 5008
R. L. Derr 2
Naval Weapons Center
China Lake, CA 93555

Director
Attn: Technical Information Section 2
Naval Research Laboratory
Washington, DC 20375

Office of Chief of Naval Operations
Operations Evaluation Group (OP03EG)
Washington, DC 20350

Director
Office of the Secretary of Defense
Advanced Research Projects Agency
Washington, DC 20301

Scientific and Technical
Information Facility, NASA
P. O. Box 33
College Park, MD 20740

Commanding Officer
Attn: R&D Division
Code 50
Naval Weapons Station
Yorktown, VA 23691

Commanding Officer
Attn: Technical Library
Naval Propellant Plant
Indian Head, MD 20640

Commanding Officer
Attn: Information Services
Naval Explosive Ordnance Disposal Facility
Indian Head, MD 20640

DISTRIBUTION (Cont.)

Copies

McDonnell Aircraft Company
Attn: M. L. Schimmel
P. O. Box 516
St. Louis, MO 63166

Commanding Officer
Naval Ammunition Depot
Crane, IN 47522

Commanding Officer
Attn: LA 151-Technical Library
Naval Underwater Systems Center
Newport, RI 02840

Commanding Officer
Attn: Code AT-7
Naval Weapons Evaluation Facility
Kirtland Air Force Base
Albuquerque, NM 87117

Commanding Officer
Attn: QEL
Naval Ammunition Depot
Concord, CA 94522

Superintendent Naval Academy
Attn: Library
Annapolis, MD 21402

Naval Plant Representative Office
Attn: SPL-332 (R. H. Guay)
Strategic Systems Project Office
Lockheed Missiles and Space Company
P. O. Box 504
Sunnyvale, CA 94088

Hercules Incorporated
Attn: Library
Allegany Ballistics Laboratory
P. O. Box 210
Cumberland, MD 21502

AMCRD
5001 Eisenhower Avenue
Alexandria, VA 22302

DISTRIBUTION (Cont.)

	Copies
Redstone Scientific Information Center Attn: Chief, Documents U. S. Army Missile Command Redstone Arsenal, AL 35809	2
Commanding Officer Attn: SARPA-TS-S #59 Picatinny Arsenal Dover, NJ 07801	
Commanding General Attn: BRL Aberdeen Proving Ground, MD 21005	
Commanding Officer Attn: Library Harry Diamond Laboratories 2800 Powder Mill Road Adelphi, MD 20783	
Armament Development & Test Center DLOSL/Technical Library Eglin Air Force Base Florida 32542	
Commanding Officer Naval Ordnance Station Louisville, KY 40124	
Director Attn: Library Applied Physics Laboratory Hopkins Road Laurel, MD 20810	
Energy Research and Development Administration Attn: DMA Washington, DC 20545	
Director Defense Nuclear Agency Washington, DC 20305	

DISTRIBUTION (Cont.)

Copies

Research Director
Attn: R. W. Van Dolah
Pittsburgh Mining and Safety
Research Center
Bureau of Mines
4800 Forbes Avenue
Pittsburgh, PA 15213

Defense Documentation Center
Cameron Station
Alexandria, VA 22314 12

Goddard Space Flight Center, NASA
Glenn Dale Road
Greenbelt, MD 20771

Lawrence Livermore Laboratory
Attn: M. Finger
E. James
E. Lee
University of California
P. O. Box 808
Livermore, CA 94551

Sandia Laboratories
Attn: R. J. Lawrence, Div. 5166
P. O. Box 5800
Albuquerque, NM 87115

Director
Attn: Library
L. C. Smith
B. G. Craig
A. Popolato
Los Alamos Scientific Laboratory
P. O. Box 1663
Los Alamos, NM 87544

DDESB
Forrestal Building, Room GS 270
Washington, DC 20314

Aerojet Ordnance and Manufacturing
Company
9236 East Hall Road
Downey, CA 90241

DISTRIBUTION (Cont.)

Copies

Hercules Incorporated Research Center
Attn: Technical Information Division
B. E. Clouser
Wilmington, DE 19899

Thiokol/Huntsville Division
Attn: Technical Library
Huntsville, AL 35807

Shock Hydrodynamics Division
Attn: Dr. L. Zernow 2
Whittaker Corporation
4716 Vineland Avenue
North Hollywood, CA 91602

Stanford Research Institute
Attn: D. Curran
C. M. Tarver
333 Ravenswood Avenue
Menlo Park, CA 94025

Thiokol/Wasatch Division
Attn: Technical Library
P. O. Box 524
Brigham City, UT 84302

Thiokol/Elkton Division
Attn: Technical Library
P. O. Box 241
Elkton, MD 21921

Teledyne McCormick Selph
P. O. Box 6
Hollister, CA 95023

Lockheed Missiles and Space Division
1122 Jagels Road
Sunnyvale, CA 94086

R. Stresau Laboratory, Inc.
Star Route
Spooner, WI 54801

DISTRIBUTION (Cont.)

Copies

Rohm and Haas
Attn: H. M. Shuey
Huntsville, Defense Contract Office
723-A Arcadia Circle
Huntsville, AL 35801

U. S. Army Foreign Service
and Technology Center
220 7th Street, N. E.
Charlottesville, VA 22901

Princeton University
Attn: M. Summerfield
Department of Aerospace and
Mechanical Sciences
Princeton, NJ 08540

Pennsylvania State University
Attn: K. Kuo
Department of Mechanical Engineering
University Park, PA 16802

Ballistic Research Laboratories
Attn: N. Gerri
Aberdeen Proving Ground, MD 21005

Paul Gough Associates
1048 South Street
Portsmouth, NH 03801

Hercules Incorporated, Bacchus Works
Attn: M. Beckstead
P. O. Box 98
Magna, UT 84044

Professor H. Krier
A & A Engineering Department
101 Transporation Building
University of Illinois
Urbana, IL 61801

Chemical Propulsion Information Agency
The Johns Hopkins University
Applied Physics Laboratory
Johns Hopkins Road
Laurel, MD 20810

DISTRIBUTION (Cont.)

Copies

IIT Research Institute
Attn: H. S. Napadensky
10 W 35th Street
Chicago, IL 60616

Erion Associates, Inc.
Attn: W. Petray
600 New Hampshire Avenue,
Suite 870
Washington, DC 20037

NSWC(W)-5605/1 (Rev. 1-75)

TO AID IN UPDATING THE DISTRIBUTION LIST FOR NAVAL SURFACE WEAPONS CENTER, WHITE OAK LABORATORY TECHNICAL REPORTS PLEASE COMPLETE THE FORM BELOW:

TO ALL HOLDERS OF NSWC/WOL TR 77-96
by Donna Price, Code CR-10

DO NOT RETURN THIS FORM IF ALL INFORMATION IS CURRENT

A. FACILITY NAME AND ADDRESS *(OLD) (Show Zip Code)*

NEW ADDRESS *(Show Zip Code)*

B. ATTENTION LINE ADDRESSES:

C.

☐ REMOVE THIS FACILITY FROM THE DISTRIBUTION LIST FOR TECHNICAL REPORTS ON THIS SUBJECT.

D.

NUMBER OF COPIES DESIRED: _____

DEPARTMENT OF THE NAVY
NAVAL SURFACE WEAPONS CENTER
WHITE OAK, SILVER SPRING, MD. 20910

OFFICIAL BUSINESS
PENALTY FOR PRIVATE USE, $300

POSTAGE AND FEES PAID
DEPARTMENT OF THE NAVY
DOD 314

COMMANDER
NAVAL SURFACE WEAPONS CENTER
WHITE OAK, SILVER SPRING, MARYLAND 20910

ATTENTION: CODE CR-10